Article

Not peer-reviewed version

Geometric Suppression of the Electroweak Scale from Calabi–Yau Singularities

Deep Bhattacharjee *, Priyanka Samal, Riddhima Sadhu, Sanjeevan Singha Roy *

Posted Date: 12 March 2026

doi: 10.20944/preprints202603.0916.v1

Keywords: hierarchy problem; Calabi–Yau compactification; geometric suppression mechanism; string phenomenology; Kaluza–Klein gravitons; D-brane instantons; moduli stabilisation; electroweak scale

 doi:10.20944/preprints202603.0916.v1

Article

Geometric Suppression of the Electroweak Scale from Calabi–Yau Singularities

Deep Bhattacharjee[1,*], Priyanka Samal[2], Riddhima Sadhu[3] and Sanjeevan Singha Roy[3,*]

[1] Electro-Gravitational Space Propulsion Laboratory (EGSPL), Odisha, India
[2] Researcher in Theoretical Physics, Odisha, India
[3] Birla Institute of Technology (former student), BIT Mesra, Jharkhand, India
* Correspondence: itsdeep@live.com (D.B.); sanjeevan9905@gmail.com (S.S.R.)

Abstract

The hierarchy problem—the seventeen-order-of-magnitude separation between the electroweak scale and the Planck scale—remains one of the most compelling open questions in theoretical physics. Within the Standard Model, quadratically divergent quantum corrections to the Higgs mass require extraordinary fine-tuning at every loop order, with no underlying physical explanation. We propose a geometric suppression mechanism in which the electroweak scale arises naturally from the local curvature geometry of singular cycles within a six-dimensional Calabi–Yau compactification of Type IIB superstring theory. When toroidal cycles degenerate, string-theoretic D-brane defects form at the resulting singular loci, and monopole-brane recoil governed by the Nambu–Goto action produces massless spin-2 gravitons that propagate into the higher-dimensional bulk. The local singularity energy density, controlled entirely by the curvature scale of the collapsed cycle, determines the electroweak mass scale without free parameters. A complementary brane-instanton mechanism generates the hierarchy exponentially from a geometric action of order thirty-seven, naturally reproducing the observed ratio of electroweak to Planck scales. We derive an explicit four-dimensional effective action from Kaluza–Klein reduction, demonstrate three independent consistency limits, compare the mechanism with Randall–Sundrum warped geometry and supersymmetric approaches, and outline a programme for embedding the proposal in explicit compactification models.

Keywords: hierarchy problem; Calabi–Yau compactification; geometric suppression mechanism; string phenomenology; Kaluza–Klein gravitons; D-brane instantons; moduli stabilisation; electroweak scale

PACS: J11.25.–w; 11.25.Mj; 04.50.–h

MSC: 83E30 (Primary); 81T30, 53C29 (Secondary)

1. Notation and Conventions

Throughout this work we use natural units $\hbar = c = 1$. The spacetime signature is $(-,+,+,+,\dots)$. Capital Latin indices $M, N, \dots$ run over all $4+n$ dimensions; Greek indices $\mu, \nu, \dots$ run over the four large dimensions; lower-case Latin indices $m, n, \dots$ run over the n compact dimensions. The reduced Planck mass is $M_{\rm Pl} = (8\pi G_N)^{-1/2} \approx 2.4 \times 10^{18}\,\text{GeV}$.

 doi:10.20944/preprints202603.0916.v1

2. Introduction

2.1. The Hierarchy Problem in Particle Physics

The Standard Model of particle physics (SM) is one of the most precisely tested theories in the history of science. Developed through the 1960s and 1970s by Glashow, Weinberg, Salam, and many others, it describes the electromagnetic, weak, and strong interactions in terms of a gauge theory with group $SU(3)_c \times SU(2)_L \times U(1)_Y$, spontaneously broken to $SU(3)_c \times U(1)_{\mathrm{em}}$ by the vacuum expectation value of the Higgs doublet field H. The discovery of the Higgs boson at the Large Hadron Collider (LHC) in 2012 [21,22] with mass $m_H \approx 125\,\mathrm{GeV}$ completed the particle content of the SM, confirming the mechanism of electroweak symmetry breaking.

Yet despite its experimental successes, the SM contains an acute internal theoretical tension: the electroweak scale $M_{\mathrm{EW}} \sim v_H/\sqrt{2} \approx 174\,\mathrm{GeV}$, set by the Higgs mechanism, and the Planck scale $M_{\mathrm{Pl}} \sim 2.4 \times 10^{18}\,\mathrm{GeV}$, set by Newton's gravitational constant $G_N = M_{\mathrm{Pl}}^{-2}$, differ by approximately seventeen orders of magnitude:

$$\frac{M_{\mathrm{EW}}}{M_{\mathrm{Pl}}} \sim 10^{-17}. \tag{1}$$

This enormous separation is not merely an observational coincidence: it creates a severe *fine-tuning problem* within quantum field theory.

Radiative instability of the Higgs mass.

The Higgs mass parameter m_H^2 in the SM Lagrangian $\mathcal{L} \supset -m_H^2|H|^2$ receives quadratically divergent radiative corrections at each loop order. At one loop, the dominant contributions come from the top quark, the W and Z bosons, and the Higgs itself:

$$\delta m_H^2 = \frac{\Lambda_{\mathrm{UV}}^2}{16\pi^2}\left[-6y_t^2 + \frac{9}{2}g^2 + \frac{3}{2}g'^2 + 3\lambda\right] + \mathcal{O}\left(\Lambda_{\mathrm{UV}}^0\right), \tag{2}$$

where $y_t \approx 1$ is the top Yukawa coupling, g and g' are the $SU(2)_L$ and $U(1)_Y$ gauge couplings, and λ is the Higgs quartic self-coupling. If the ultraviolet cutoff is taken to be the Planck scale, $\Lambda_{\mathrm{UV}} = M_{\mathrm{Pl}}$, then $\delta m_H^2 \sim (10^{18}\,\mathrm{GeV})^2 \approx 10^{36}\,\mathrm{GeV}^2$, while the physical value is $m_H^2 \approx (125\,\mathrm{GeV})^2 \approx 1.6 \times 10^4\,\mathrm{GeV}^2$. The ratio $\delta m_H^2/m_H^2 \approx 10^{32}$ measures the degree of cancellation required between the bare mass parameter and the radiative corrections. This cancellation must occur at *every* order of perturbation theory and must be maintained under renormalisation group running—a condition of extraordinary delicacy that has no physical explanation within the SM.

The naturalness criterion.

The concept of *naturalness* [19] provides a precise formulation of the problem. A theory is said to be natural if all dimensionless parameters are of order unity, or more precisely if a parameter is small only when its smallness is protected by an enhanced symmetry of the theory in the limit where the parameter vanishes. The Higgs mass does not satisfy this criterion: in the limit $m_H \to 0$, the SM does not acquire any new symmetry, and consequently radiative corrections drive m_H^2 to the largest available scale in the theory. The observed value $m_H \approx 125\,\mathrm{GeV} \ll M_{\mathrm{Pl}}$ is therefore unnatural from the perspective of quantum field theory with a Planck-scale ultraviolet completion.

The hierarchy in supersymmetry and beyond.

It is important to distinguish the hierarchy problem from the related but distinct question of the cosmological constant problem. The latter concerns the vacuum energy density of the universe, which

 doi:10.20944/preprints202603.0916.v1

is observed to be of order $(10^{-3}\,\mathrm{eV})^4$ but receives quantum corrections of order Λ_{UV}^4—an even more severe fine-tuning. The hierarchy problem is specifically about the Higgs mass and the electroweak scale; any complete solution must explain why $m_H^2 \ll M_{\mathrm{Pl}}^2$ without extreme cancellations. Several classes of solutions have been proposed over the past four decades, and we review the most prominent ones in Section 2.2.

2.2. Existing Proposed Solutions

2.2.1. Supersymmetry

Supersymmetry (SUSY) [10,20] is the most extensively studied solution to the hierarchy problem. It posits a symmetry between bosons and fermions such that for every SM particle of spin s there exists a superpartner of spin $s \pm 1/2$. Because bosonic and fermionic loops contribute with opposite signs to radiative corrections, the quadratic divergences cancel:

$$\delta m_H^2\big|_{\mathrm{SUSY}} = \frac{\Lambda_{\mathrm{UV}}^2}{16\pi^2}\left[\left(-6y_t^2 + 6\tilde{y}_t^2\right) + \cdots\right] = 0 \quad (\text{exact SUSY}), \tag{3}$$

where $\tilde{y}_t$ denotes the stop squark Yukawa coupling equal to y_t by supersymmetry. When SUSY is softly broken at a scale M_{soft}, the residual correction is of order $\delta m_H^2 \sim M_{\mathrm{soft}}^2 \ln(\Lambda_{\mathrm{UV}}/M_{\mathrm{soft}})$, which is naturally of order m_H^2 provided $M_{\mathrm{soft}} \lesssim$ TeV.

However, supersymmetry has not been observed experimentally. LHC searches have placed lower bounds on squark and gluino masses in the multi-TeV range [23,24], pushing M_{soft} well above the electroweak scale and reintroducing a little hierarchy problem. Furthermore, SUSY does not explain the *origin* of M_{soft}: it transfers the fine-tuning problem to the mechanism of SUSY breaking, which requires additional model-building. Finally, in the minimal supersymmetric SM (MSSM), the predicted Higgs mass is at most $m_h \lesssim m_Z \approx 91\,\mathrm{GeV}$ at tree level; reproducing $m_H \approx 125\,\mathrm{GeV}$ requires large radiative corrections, reintroducing fine-tuning at the percent level.

2.2.2. Composite Higgs and Technicolour

In composite Higgs models [26,27], the Higgs boson is not an elementary scalar but a pseudo-Nambu–Goldstone boson (pNGB) arising from the spontaneous breaking of a global symmetry $\mathcal{G} \to \mathcal{H}$ at a scale f. The Higgs mass is then technically natural because a shift symmetry protects it; the corrections are of order $\delta m_H^2 \sim g_*^2 f^2/(16\pi^2)$ where g_* is a typical strong coupling. For $f \sim$ few TeV, this gives $m_H^2 \sim (100\,\mathrm{GeV})^2$, consistent with observation. The price is the prediction of a spectrum of heavy resonances at scales $m_\rho \sim g_* f$, which must have escaped LHC detection. Current constraints from composite resonance searches push $f \gtrsim 1\,\mathrm{TeV}$, implying at least a 10% fine-tuning in the Higgs potential [33].

Technicolour models [28,29] replaced the Higgs field entirely with a strongly-coupled condensate, but this approach was effectively ruled out by precision electroweak measurements at LEP, particularly the S and T oblique correction parameters. Modern extended technicolour and walking technicolour variants survive some of these constraints but face similar difficulties with fermion mass generation.

2.2.3. Extra Dimensions: The ADD Mechanism

The Arkani-Hamed–Dimopoulos–Dvali (ADD) framework [1,2] takes a radically different approach: rather than cancelling the radiative corrections to the Higgs mass, it redefines the fundamental scale of

 doi:10.20944/preprints202603.0916.v1

gravity. If there exist n extra spatial dimensions compactified on a torus of radius R, then Newton's law in $(4+n)$ dimensions gives $G_{4+n} \sim G_N / V_n$ where $V_n = R^n$, and Gauss's law implies

$$M_{\rm Pl}^2 = M_*^{2+n}\, V_n. \tag{4}$$

If $M_* \sim$ TeV, then the observed $M_{\rm Pl} \sim 10^{18}\,$GeV is a derived quantity, not a fundamental scale. The hierarchy $M_{\rm EW}/M_{\rm Pl}$ is then explained as a consequence of the large volume $V_n = (M_{\rm Pl}/M_*)^{2/n} M_*^{-n}$: for $n = 2$, $R \sim 0.1\,$mm; for $n = 6$, $R \sim 10^{-14}\,$m.

The ADD mechanism has several attractive features: it requires no new particles at the electroweak scale, it has concrete experimental signatures (missing energy from KK graviton emission at the LHC [12], deviations from Newton's law at sub-millimetre scales [11]), and it connects naturally to string compactification. However, it does not explain the electroweak scale itself—the ratio $M_{\rm EW}/M_*$ remains an external input. The mechanism explains why gravity is weak ($M_{\rm Pl} \gg M_*$) but not why $M_{\rm EW} \sim M_*$.

2.2.4. Randall–Sundrum Warped Geometry

Randall and Sundrum [3,4] proposed an alternative in which the extra dimension is curved (warped) rather than flat. In the RS1 model, two 3-branes (the UV or Planck brane and the IR or TeV brane) sit at the boundaries of a five-dimensional Anti-de Sitter (AdS_5) spacetime with metric

$$ds^2 = e^{-2k|y|}\eta_{\mu\nu}dx^\mu dx^\nu + dy^2, \tag{5}$$

where k is the AdS curvature scale and y is the coordinate of the extra dimension with $y \in [0, \pi r_c]$. The exponential warp factor $e^{-k|y|}$ generates an exponential hierarchy: if all fundamental scales on the UV brane are of order $M_{\rm Pl}$, then the physical mass scales on the IR brane are suppressed by $e^{-k\pi r_c}$. Requiring $e^{-k\pi r_c} \sim 10^{-15}$ fixes $kr_c \approx 12$, a modest number requiring no extreme fine-tuning. The Goldberger–Wise mechanism [31] stabilises the brane separation r_c through a bulk scalar field with boundary potentials.

The RS mechanism is elegant and predictive: it yields a discrete spectrum of KK graviton resonances at $\mathcal{O}(\text{TeV})$ potentially observable at the LHC, and the zero-mode graviton is exponentially localised near the UV brane. Its limitations are that it is a five-dimensional construction not obviously embedded in string theory, and the electroweak scale is still fixed by hand through the brane separation rather than derived from first principles.

2.2.5. The Relaxion

The relaxion [30] is a more recent proposal in which the Higgs mass scans dynamically during inflation. A new axion-like field ϕ (the relaxion) rolls down a potential $V(\phi) \sim -g\phi\Lambda^2 + \Lambda^4$, where Λ is the UV cutoff, causing the Higgs mass $m_H^2(\phi) \sim \Lambda^2 - g\phi\Lambda^2/\Lambda^2$ to decrease. When m_H^2 changes sign, electroweak symmetry is broken, backreaction from the Yukawa sector generates a back-potential, and ϕ is trapped at a value giving the small observed Higgs mass. The relaxion elegantly exploits classical dynamics to scan the landscape of Higgs masses, but it requires a very flat potential (technically from the axion periodicity), a suitable inflationary history, and introduces new parameters.

2.3. Limitations of Supersymmetry

As the most developed solution to the hierarchy problem, supersymmetry deserves a more detailed critical assessment. The Minimal Supersymmetric Standard Model (MSSM) adds to the SM spectrum a complete supersymmetric partner for every SM field: squarks $\tilde{q}_{L,R}$, sleptons $\tilde{l}_{L,R}$, gauginos $\tilde{g}, \tilde{W}, \tilde{B}$, Higgsinos $\tilde{H}_{u,d}$, and two Higgs doublets H_u, H_d. The soft-breaking sector introduces $\mathcal{O}(100)$ new

 doi:10.20944/preprints202603.0916.v1

parameters, most of which are constrained by flavour physics and CP violation. At the most fundamental level, SUSY has three categories of limitations relevant to the hierarchy problem.

The μ-problem.

The MSSM superpotential contains the term $\mu H_u H_d$ where μ is a dimensionful parameter with mass dimension one. Phenomenological consistency (electroweak symmetry breaking, chargino masses) requires $\mu \sim m_Z$, but there is no symmetry in the MSSM that enforces $\mu \sim M_{\text{soft}} \sim m_Z$ rather than $\mu \sim M_{\text{Pl}}$. This is the μ-problem [35]: SUSY reintroduces a fine-tuning in the superpotential. Various solutions (the NMSSM, Giudice–Masiero mechanism) require additional structure.

The little hierarchy.

Non-observation of superpartners at the LHC currently implies $m_{\tilde{g}} \gtrsim 2.2\,\text{TeV}$ and $m_{\tilde{q}} \gtrsim 1.5$–$2\,\text{TeV}$ for first- and second-generation squarks [23]. With such heavy superpartners, the radiative correction to m_H^2 is

$$\delta m_H^2 \approx -\frac{3y_t^2}{8\pi^2} m_{\tilde{t}}^2 \ln\left(\frac{\Lambda}{m_{\tilde{t}}}\right) \approx -(500\,\text{GeV})^2 \quad (m_{\tilde{t}} \sim 2\,\text{TeV}), \tag{6}$$

which already exceeds m_H^2 by a factor of ~ 16. This *little hierarchy problem* suggests that even if SUSY is correct, a residual percent-level fine-tuning remains [34].

SUSY breaking.

The mechanism of SUSY breaking is not determined within the MSSM. Gravity-mediated breaking (mSUGRA), gauge-mediated breaking (GMSB), and anomaly-mediated breaking (AMSB) each lead to qualitatively different phenomenologies and each introduces additional model-dependence. None of these mechanisms derives $M_{\text{soft}} \sim M_{\text{EW}}$ from first principles; they merely parameterise our ignorance of SUSY breaking.

Experimental status.

After Run 1 and Run 2 of the LHC, no evidence for supersymmetric particles has been found in any channel. Naturalness arguments that motivated TeV-scale SUSY as the most likely new physics at the LHC have been systematically falsified by null results. While SUSY remains a theoretically attractive framework for unification and string phenomenology, its ability to *solve* the hierarchy problem without residual fine-tuning is in serious tension with current data.

2.4. Warped Extra Dimensions: Randall–Sundrum and Its Limitations

The RS mechanism has been enormously influential and deserves detailed examination of both its virtues and limitations. The exponential warp factor provides a compelling geometric explanation of the hierarchy: starting from $\mathcal{O}(M_{\text{Pl}})$ mass scales on the UV brane, physical scales on the IR brane are red-shifted by $e^{-k\pi r_c}$. For $k \approx M_{\text{Pl}}$ and r_c of order $10\,k^{-1}$, the electroweak scale $M_{\text{EW}} \sim M_{\text{Pl}} e^{-k\pi r_c}$ is naturally generated.

However, the RS model has structural limitations. First, it is an effective five-dimensional theory; its ultraviolet completion in string theory is not straightforward. Randall–Sundrum geometries arise as specific backgrounds in Type IIB string theory with orientifold planes, but the moduli stabilisation in such setups is non-trivial and generically leads to corrections to the warp factor. Second, the Goldberger–Wise stabilisation mechanism, while technically natural, relies on a bulk scalar with specific boundary conditions that must be tuned to give the observed hierarchy. Third, the KK spectrum of the RS model is

 doi:10.20944/preprints202603.0916.v1

qualitatively different from that of flat extra dimensions: the KK graviton masses are not equally spaced ($m_n \sim x e^{-k\pi r_c} M_{\rm Pl}/\pi$ where x_n are zeros of Bessel functions), and the coupling of KK gravitons to SM fields is enhanced by $1/(M_{\rm Pl} e^{-k\pi r_c}) \sim 1/\text{TeV}$. LHC searches for spin-2 KK graviton resonances have placed lower bounds $m_{\rm KK} \gtrsim 4$–$5\,\text{TeV}$ for $k/\overline{M_{\rm Pl}} > 0.1$ [25]. Fourth, and most relevantly for the present work, the RS mechanism operates in five dimensions and does not exploit the rich geometric structure of Calabi–Yau threefolds.

2.5. String Compactifications and the Hierarchy

String theory provides the most complete framework for addressing the hierarchy problem because it unifies gravity with gauge interactions in a consistent ultraviolet-complete quantum theory. The ten-dimensional superstring is compactified on a six-dimensional internal manifold $\mathcal{M}_6$ to produce a four-dimensional effective theory. The properties of this effective theory—its gauge group, matter content, Yukawa couplings, and mass scales—are determined entirely by the geometry and topology of $\mathcal{M}_6$.

The most extensively studied class of compactification manifolds are the Calabi–Yau threefolds [5]: compact Kähler manifolds of $SU(3)$ holonomy with vanishing first Chern class. Their special holonomy ensures that the internal geometry preserves $\mathcal{N} = 1$ supersymmetry in four dimensions (starting from $\mathcal{N} = 1$ in ten dimensions for the heterotic string, or $\mathcal{N} = 2$ for Type II theories before orientifolding). The rich moduli space of Calabi–Yau manifolds—parameterised by the Kähler moduli controlling the sizes of internal cycles and the complex structure moduli controlling their shapes—provides a vast landscape of possible four-dimensional vacua.

Stabilising these moduli is a central challenge. The GKP construction [6] showed that background Ramond–Ramond and Neveu–Schwarz three-form fluxes F_3 and H_3 generate a superpotential $W_0 = \int_{\mathcal{M}_6} G_3 \wedge \Omega$ that stabilises all complex structure moduli. KKLT [7] added non-perturbative corrections (from gaugino condensation or Euclidean D3-brane instantons) to stabilise the Kähler moduli, producing a metastable de Sitter vacuum after uplifting. The Large Volume Scenario (LVS) [32] provides an alternative stabilisation with the compactification volume exponentially large in string units, naturally producing $M_{\rm Pl} \gg M_s$.

Despite this progress, the origin of the electroweak scale within string compactifications has remained obscure. The GKP/KKLT programme can stabilise moduli and generate an exponentially small superpotential $W_0 \sim e^{-2\pi/g_s}$, which after SUSY breaking could seed $M_{\rm EW}$, but this route relies on the landscape statistical argument and does not provide a geometric derivation from specific compactification data.

2.6. Why Calabi–Yau Singularities?

The central observation motivating the present work is that Calabi–Yau singularities—points or loci in the compact space where the metric degenerates—carry a finite, localised energy density that is entirely determined by the local geometry. This energy density has the correct parametric dependence to generate the electroweak scale from the Planck scale without fine-tuning.

A Calabi–Yau singularity arises when a cycle in the compact space collapses to zero size. The simplest example is the conifold singularity [17,37], at which a topological S^3 collapses; the resolved conifold replaces it with an S^2 of finite size. Near such a singularity, the local geometry is a cone over a compact manifold ($T^{1,1} = SU(2) \times SU(2)/U(1)$ for the conifold), and the metric diverges in a controlled way characterised by a single length scale $R_{\rm sing}$.

In the string-theoretic context, Strominger [17] showed that the singularity of the conifold can be resolved by wrapping D3-branes on the collapsing S^3, which become massless at the singularity and

 doi:10.20944/preprints202603.0916.v1

correspond to new light degrees of freedom in the four-dimensional theory. The tension of the wrapped brane is $T_{\text{wrapped}} \sim T_{D3}\text{Vol}(S^3)$, and at the singularity $\text{Vol}(S^3) \to 0$, so the brane becomes massless. This mechanism was the first example of a geometry-induced mass scale in string theory.

The mechanism proposed in the present work is the converse: rather than sending $\text{Vol}(\Sigma) \to 0$ and producing massless states, we consider the case in which $\text{Vol}(\Sigma) \sim \mathcal{O}(10\text{–}20)\ell_s^2$ is small but finite, so that the instanton action $S_{\text{geom}} = \text{Vol}(\Sigma)/(g_s\ell_s^2)$ is of order 37, naturally generating the hierarchy $e^{-37} \sim 10^{-16}$. The singularity is not fully collapsed but is near-singular; the local curvature scale R_{sing} is small in Planck units, encoding the ratio $M_{\text{EW}}/M_{\text{Pl}}$ in the geometry of the compact space.

This geometric interpretation suggests that the hierarchy problem is not a problem of fine-tuning within a fixed theory, but rather a consequence of the topology and geometry of the compactification: the electroweak scale is a geometric datum, as fundamental as the Kähler moduli of the Calabi–Yau.

2.7. Summary of Main Contributions

The present work derives the following results from Calabi–Yau singularity geometry and string brane dynamics.

- **Planck scale from compactification.** Dimensional reduction of the $(4+6)$-dimensional Einstein–Hilbert action over the Calabi–Yau volume $V_6 = R^6$:

$$M_{\text{Pl}}^2 = M_*^8\, V_6. \tag{7}$$

- **Electroweak scale from singularity energy density.** The $D-1$ brane defect at the degenerated torus cycle carries tension $T_{D-1} \sim M_s^2/g_s$ and fills a singular volume $V_{\text{sing}} \sim R_{\text{sing}}^3$, giving

$$M_{\text{EW}}^2 \approx \frac{\rho_{\text{CY}}}{M_{\text{Pl}}}, \qquad \rho_{\text{CY}} = \frac{T_{D-1}}{V_{\text{sing}}} \sim \frac{M_s^2}{g_s R_{\text{sing}}^3}. \tag{8}$$

- **Higgs vacuum expectation value.** The curvature scale $\Lambda_{\text{CY}}^2 = R_{\text{sing}}^{-2}$ of the CY singularity sets:

$$v_{\text{Higgs}} \sim \frac{\Lambda_{\text{CY}}^2}{M_{\text{Pl}}} \approx 246\,\text{GeV}. \tag{9}$$

- **Exponential suppression.** A wrapped-brane instanton with action $S_{\text{geom}} \approx 37$ gives:

$$M_{\text{EW}} \sim M_{\text{Pl}}\, e^{-S_{\text{geom}}}, \qquad \frac{M_{\text{EW}}}{M_{\text{Pl}}} \sim 10^{-16}. \tag{10}$$

- **Dynamical compactification.** A modulus potential $V(R) = A/R^4 + BR^2 + C$ stabilises the compactification radius at $R \approx 10^{-14}\,\text{m}$.
- **Kaluza–Klein spectrum.** $m_{\text{KK}} \approx n/R$ with first mode mass $\approx 30\,\text{MeV}$.

 doi:10.20944/preprints202603.0916.v1

2.8. Scope, Assumptions, and Outline

Central Result of This Work

The central claim of this paper is that the electroweak hierarchy is a *geometric datum*—a consequence of the topology of the Calabi–Yau compactification rather than an accident requiring fine-tuning.
The mechanism rests on two complementary observations. First, when a toroidal cycle in the compact space degenerates, a localised energy density $\rho_{\mathrm{CY}} \sim M_*^2/(g_s R_{\mathrm{sing}}^3)$ is generated at the resulting singularity. The ratio of this density to the Planck mass precisely sets the electroweak scale: $M_{\mathrm{EW}}^2 \approx \rho_{\mathrm{CY}}/M_{\mathrm{Pl}}$. The Higgs vacuum expectation value $v_{\mathrm{Higgs}} \approx 246\,\mathrm{GeV}$ then follows from the singularity curvature scale via $v_{\mathrm{Higgs}} \sim \Lambda_{\mathrm{CY}}^2/M_{\mathrm{Pl}}$—connecting the observed electroweak scale directly to the local geometry of the compact space.
Second, a D-brane instanton wrapping a cycle of modest volume ($\approx$ 15–18 string lengths squared) near the singularity generates an exponential factor $e^{-S_{\mathrm{geom}}}$ with $S_{\mathrm{geom}} \approx 37$. This single number, fixed entirely by the compactification geometry, reproduces the observed ratio $M_{\mathrm{EW}}/M_{\mathrm{Pl}} \sim 10^{-16}$ without any parameter tuning. The hierarchy is not imposed; it is a consequence of the local curvature of extra dimensions.

The analysis rests on the following assumptions, each standard in string compactification phenomenology.

1. **Local CY geometry approximation.** A closed-form Ricci-flat metric on a compact CY manifold is not available; we use a local expansion $g_{mn} = g_{mn}^{(0)} + h_{mn}$ valid near the singularity, where $R_{mn}(g^{(0)}) = 0$.
2. **Effective brane tension.** The $D-1$ brane tension is taken to be $T_{D-1} \sim M_s^2/g_s$, the leading-order string-theoretic estimate; higher-order α' corrections are neglected.
3. **Perturbative string coupling.** We assume $g_s < 1$ throughout, so that the string perturbation series is under control.
4. **Large-volume compactification.** The compactification satisfies $M_* R \gg 1$, validating the effective field theory description.

The paper is organised as follows. Section 3 reviews the mathematical background: differential geometry, Ricci-flat manifolds, Calabi–Yau geometry, singularity structures, and moduli spaces. Section 4 presents the string compactification framework and the emergence of the effective field theory. Section 5 describes the geometric setup. Section 6 explains the monopole-brane mechanism. Section 7 provides the mathematical derivations. Section 8 derives the effective field theory. Section 9 discusses brane topology and flux contributions. Section 10 constructs a toy compactification model. Sections 11, 12 and 14 present the main theorem, naturalness argument, and phenomenological predictions. Section 13 compares with other mechanisms. Section 15 provides numerical estimates. Sections 16, 17, 19 and 20 discuss consistency, comparison, future directions, and conclusions. Appendices A–E provide technical details.

3. Mathematical Foundations

3.1. Differential Geometry: Connections and Curvature

We briefly review the differential geometry relevant to Calabi–Yau compactification. Let (M, g) be a smooth Riemannian manifold of real dimension $2n$ (for a Calabi–Yau threefold, $n = 3$ and the real dimension is six).

 doi:10.20944/preprints202603.0916.v1

Connections and covariant derivatives.

The Levi-Civita connection is the unique torsion-free connection compatible with the metric g:

$$\Gamma^{\rho}_{\mu\nu} = \frac{1}{2} g^{\rho\sigma} \left(\partial_\mu g_{\nu\sigma} + \partial_\nu g_{\mu\sigma} - \partial_\sigma g_{\mu\nu} \right). \tag{11}$$

The Riemann curvature tensor is defined by

$$R^{\rho}{}_{\sigma\mu\nu} = \partial_\mu \Gamma^{\rho}_{\nu\sigma} - \partial_\nu \Gamma^{\rho}_{\mu\sigma} + \Gamma^{\rho}_{\mu\lambda} \Gamma^{\lambda}_{\nu\sigma} - \Gamma^{\rho}_{\nu\lambda} \Gamma^{\lambda}_{\mu\sigma}. \tag{12}$$

Contracting on two indices yields the Ricci tensor:

$$R_{\mu\nu} = R^{\rho}{}_{\mu\rho\nu}, \tag{13}$$

and further contraction gives the Ricci scalar $\mathcal{R} = g^{\mu\nu} R_{\mu\nu}$.

Holonomy.

Given a connection on M, parallel transport around a closed loop generally returns a vector rotated by an element of the *holonomy group* $\mathrm{Hol}(M, g) \subseteq O(2n)$. For an irreducible Riemannian manifold, Berger's classification theorem [36] lists all possible restricted holonomy groups. For Kähler manifolds the holonomy is contained in $U(n)$, and for Calabi–Yau manifolds (Ricci-flat Kähler) the holonomy is exactly $SU(n)$—a crucial distinction, as $SU(n) \subset U(n)$ removes the $U(1)$ factor.

3.2. Ricci-Flat Manifolds

A Riemannian manifold (M, g) is *Ricci-flat* if

$$R_{\mu\nu} = 0, \tag{14}$$

which in general relativity corresponds to the vacuum Einstein equations in the absence of a cosmological constant. Ricci-flatness is weaker than flatness (vanishing Riemann tensor) and weaker than being an Einstein manifold (proportional Ricci tensor); a Ricci-flat manifold can have non-zero Riemann curvature.

Physical significance.

In string compactification, the internal space must satisfy the supergravity equations of motion. At leading order in α', these reduce to the requirement that the internal metric be Ricci-flat [5]. This is why Calabi–Yau manifolds—Ricci-flat Kähler manifolds—are the natural choices for string compactification. The Ricci-flat condition ensures:

1. *Supersymmetry preservation:* In Type IIB on a Ricci-flat Kähler manifold, $\mathcal{N} = 2$ supersymmetry is preserved in four dimensions before orientifolding.
2. *Equations of motion:* The ten-dimensional supergravity equations of motion are satisfied at tree level.
3. *Scale separation:* The Ricci-flat condition is consistent with having hierarchically different internal and external scales.

Yau's theorem.

The central mathematical result underpinning the entire Calabi–Yau programme is Yau's theorem [13]:

 doi:10.20944/preprints202603.0916.v1

Theorem 1 (Yau 1978). *Let X be a compact Kähler manifold with vanishing first Chern class, $c_1(X) = 0$. Then for every Kähler class $[\omega] \in H^{1,1}(X, \mathbb{R})$, there exists a unique Ricci-flat Kähler metric g whose Kähler form represents $[\omega]$.*

Yau's theorem establishes *existence* and *uniqueness* but provides no explicit formula for the metric. This is why string compactifications on Calabi–Yau manifolds proceed through indirect means: one computes physical quantities (Yukawa couplings, gauge kinetic functions, moduli Kähler potential) using the topological and complex analytic structure of the CY manifold without ever writing down the metric explicitly.

3.3. Calabi–Yau Manifolds

Definition 2 (Calabi–Yau n-fold). A *Calabi–Yau n-fold* is a compact complex manifold X of complex dimension n satisfying any of the following equivalent conditions:

1. X is Kähler with holonomy group exactly $SU(n)$.
2. X is Kähler with $c_1(X) = 0$ and admits a Ricci-flat Kähler metric.
3. X is Kähler with trivial canonical bundle $K_X \cong \mathcal{O}_X$.
4. X admits a nowhere-vanishing holomorphic $(n, 0)$-form Ω.

For string compactification, the relevant case is $n = 3$, giving a Calabi–Yau threefold (CY_3) of real dimension six.

Hodge structure.

The cohomology of a CY_3 is organised by Hodge numbers $h^{p,q}$. By the holonomy constraint $\mathrm{Hol} = SU(3)$, all non-trivial Hodge numbers are determined by $h^{1,1}$ and $h^{2,1}$: the full Hodge diamond of a CY_3 is

$$\begin{array}{ccccc} & & 1 & & \\ & 0 & & 0 & \\ 0 & & h^{1,1} & & 0 \\ & h^{2,1} & & h^{2,1} & \\ 0 & & h^{1,1} & & 0 \\ & 0 & & 0 & \\ & & 1 & & \end{array} \tag{15}$$

The Euler characteristic is

$$\chi = 2(h^{1,1} - h^{2,1}). \tag{16}$$

The $h^{1,1}$ Kähler moduli parameterise the sizes of 2-cycles and 4-cycles, while the $h^{2,1}$ complex structure moduli parameterise the shapes. Both sets of moduli must be stabilised in a phenomenologically viable compactification.

Special geometry.

The moduli space of a CY_3 has a special geometric structure. The Kähler moduli space is a special Kähler manifold with prepotential

$$\mathcal{F} = d_{abc} \frac{T^a T^b T^c}{T^0}, \tag{17}$$

 doi:10.20944/preprints202603.0916.v1

where $T^a = b^a + it^a$ are complexified Kähler moduli (b^a are axions and t^a are the volumes of 2-cycles in string units), and $d_{abc} = \int_X J_a \wedge J_b \wedge J_c$ are the triple intersection numbers. The Kähler potential for these moduli is

$$\mathcal{K}_{\text{Kähler}} = -2 \ln \mathcal{V}, \tag{18}$$

where $\mathcal{V} = \frac{1}{6} \int_X J \wedge J \wedge J$ is the overall volume of X in string units.

Examples.

The most well-known Calabi–Yau threefold is the quintic hypersurface in $\mathbb{CP}^4$, defined by a degree-5 polynomial equation:

$$z_0^5 + z_1^5 + z_2^5 + z_3^5 + z_4^5 = 0 \qquad \subset \mathbb{CP}^4. \tag{19}$$

This has $h^{1,1} = 1$, $h^{2,1} = 101$, $\chi = -200$. The single Kähler modulus controls the overall volume; the 101 complex structure moduli parameterise the coefficients of the degree-5 polynomial. A one-parameter family of quintic CY manifolds was among the first to be studied in string phenomenology [5,14].

3.4. Singularity Structures in Calabi–Yau Spaces

Calabi–Yau manifolds generically develop singularities on the boundary of their moduli space. These singularities occur when the volume of some cycle shrinks to zero. Understanding the physics of these singularities is central to the present work.

The conifold.

The conifold is the simplest and most thoroughly studied CY singularity. It is defined by the complex threefold $\mathcal{C}$ in $\mathbb{C}^4$ given by

$$z_1^2 + z_2^2 + z_3^2 + z_4^2 = 0, \tag{20}$$

which has an isolated singular point at $z_i = 0$ for all i. The smooth resolved conifold $\widehat{\mathcal{C}}$ is obtained by blowing up the singularity to an $\mathbb{S}^2 \cong \mathbb{CP}^1$ of radius ϵ:

$$\widehat{\mathcal{C}} = \mathcal{O}(-1) \oplus \mathcal{O}(-1) \to \mathbb{CP}^1. \tag{21}$$

Alternatively, the deformed conifold $\check{\mathcal{C}}$ replaces the singularity with a finite $\mathbb{S}^3$: $z_1^2 + z_2^2 + z_3^2 + z_4^2 = \mu^2$. The transition between the resolved and deformed conifolds was studied by Candelas and de la Ossa [37].

Singularity resolution and the Higgs mechanism.

Strominger [17] showed that at the conifold singularity, D3-branes wrapping the collapsing $\mathbb{S}^3$ become massless. These extra massless states are not visible in the supergravity approximation and give rise to enhanced gauge symmetry, analogous to the Higgs mechanism. The mass of the wrapped brane is

$$m_{\text{D3}} = T_{D3} \, \text{Vol}(\mathbb{S}^3) \propto |\mu|, \tag{22}$$

so at $\mu = 0$ the brane is massless and a new phase transition occurs.

Orbifold singularities.

Another important class of singularities arises from orbifold constructions. The orbifold $\mathbb{C}^3/\mathbb{Z}_n$ is defined by the identification $(z_1, z_2, z_3) \sim (\omega z_1, \omega^a z_2, \omega^b z_3)$ where $\omega = e^{2\pi i/n}$ and $a + b \equiv 0 \pmod{n}$. These are Calabi–Yau singularities admitting explicit crepant resolutions. The resolved orbifold has

 doi:10.20944/preprints202603.0916.v1

$h^{1,1} = (n-1)$ Kähler moduli corresponding to the $n-1$ exceptional divisors, and the volumes of these divisors can be tuned to give small instanton actions.

Near-singular geometry and local models.

For the purposes of the present work, the crucial point is the behaviour of the metric near the singularity. In the neighbourhood of a conifold point, the metric takes the Stenzel form [38]:

$$ds^2_{\text{conifold}} = dr^2 + r^2\, ds^2_{T^{1,1}}, \tag{23}$$

where $T^{1,1} = SU(2) \times SU(2)/U(1)$ and r is the radial coordinate with $r \to 0$ at the singularity. The curvature of this metric near $r = 0$ is of order R^{-2}_{sing} where R_{sing} is the scale at which the cycle has shrunk to. This is the geometric datum that enters our derivation of the electroweak scale.

3.5. Moduli Spaces

The moduli space $\mathcal{M}$ of a CY_3 is the space of deformation parameters preserving the Calabi–Yau condition. It factorises locally as

$$\mathcal{M} \cong \mathcal{M}_{\text{Kähler}} \times \mathcal{M}_{\text{cs}}, \tag{24}$$

where $\mathcal{M}_{\text{Kähler}}$ has complex dimension $h^{1,1}$ and $\mathcal{M}_{\text{cs}}$ has complex dimension $h^{2,1}$.

Limits in moduli space.

Several limiting regions of moduli space are physically important:

- *Large volume limit:* $t^a \to \infty$ for all Kähler moduli. The compactification volume $\mathcal{V} \to \infty$ and the effective field theory description becomes valid.
- *Small volume/degeneration limit:* Some $t^a \to 0$. A cycle collapses and a singularity forms. New light states appear and the effective field theory breaks down.
- *Mirror limit:* Related by mirror symmetry to the small-volume limit of the mirror CY. The complex structure moduli $u^i \to \infty$ correspond to large-volume Kähler moduli of the mirror.

The degeneration limit is the physically relevant one for the present work. As a Kähler modulus $t^a \to 0$, the corresponding 2-cycle Σ_a collapses, and the instanton action $S_{\text{geom}} = t^a/g_s$ decreases. For the mechanism of the present paper to apply, we require $S_{\text{geom}} \approx 37$, which corresponds to $t^a \approx 18.5\, g_s \ell_s^2$ with $g_s = 0.5$, i.e., a cycle of area $\approx 18.5 \ell_s^2$—small but not at the singular boundary of moduli space.

4. String Compactification Framework

4.1. Ten-Dimensional Type IIB Supergravity

The low-energy limit of Type IIB superstring theory is ten-dimensional Type IIB supergravity. In the Einstein frame, the bosonic action is

$$S_{\text{IIB}} = \frac{1}{2\kappa_{10}^2} \int d^{10}x \sqrt{-g_{10}} \left[\mathcal{R}_{10} - \frac{|\partial\tau|^2}{2(\text{Im}\,\tau)^2} - \frac{|G_3|^2}{2\,\text{Im}\,\tau} - \frac{|\tilde{F}_5|^2}{4} \right] + S_{\text{CS}} + S_{\text{loc}}, \tag{25}$$

where $\kappa_{10}^2 = \frac{1}{2}(2\pi)^7 \alpha'^4 g_s^2$ is the ten-dimensional gravitational coupling, $\tau = C_0 + ie^{-\phi}$ is the axio-dilaton (C_0 is the RR axion, ϕ is the dilaton), $G_3 = F_3 - \tau H_3$ is the complex three-form flux ($F_3 = dC_2$ and $H_3 = dB_2$ are the RR and NS-NS three-form field strengths), $\tilde{F}_5 = F_5 - \frac{1}{2} C_2 \wedge H_3 + \frac{1}{2} B_2 \wedge F_3$ is the self-dual five-form, S_{CS} is the Chern–Simons term, and S_{loc} contains localised sources (D-branes, O-planes).

 doi:10.20944/preprints202603.0916.v1

4.2. Kaluza–Klein Reduction from 10D to 4D

We compactify the ten-dimensional theory on a CY_3 X by writing the ten-dimensional metric as a product (in the absence of warping):

$$ds_{10}^2 = g_{\mu\nu}(x)dx^\mu dx^\nu + g_{mn}(y)dy^m dy^n, \tag{26}$$

where x^μ are the four large-dimension coordinates and y^m are the six compact coordinates. The ten-dimensional Ricci scalar splits as

$$\mathcal{R}_{10} = \mathcal{R}_4 + \mathcal{R}_6, \tag{27}$$

where $\mathcal{R}_4$ is the four-dimensional curvature and $\mathcal{R}_6$ is the curvature of the internal space. For a Ricci-flat internal space, $\mathcal{R}_6 = 0$.

Integrating the ten-dimensional Einstein–Hilbert action over the compact dimensions:

$$\begin{aligned} S_{\rm EH}^{(10)} &= \frac{1}{2\kappa_{10}^2}\int d^{10}x\,\sqrt{-g_{10}}\,\mathcal{R}_{10} \\ &= \frac{V_6}{2\kappa_{10}^2}\int d^4x\,\sqrt{-g_4}\,\mathcal{R}_4 \qquad (\mathcal{R}_6 = 0), \end{aligned} \tag{28}$$

where $V_6 = \int_X \sqrt{g_6}\,d^6y$ is the volume of the compact space. Comparing with the four-dimensional Einstein–Hilbert action $S_{\rm EH}^{(4)} = \frac{M_{\rm Pl}^2}{2}\int d^4x\sqrt{-g_4}\mathcal{R}_4$, we identify

$$\boxed{M_{\rm Pl}^2 = \frac{V_6}{\kappa_{10}^2} = \frac{V_6}{\ell_s^8\,(2\pi)^7 g_s^2/2} \sim \frac{M_*^8 V_6}{(2\pi)^7/2\,g_s^2\alpha'^4}.} \tag{29}$$

In the simplified (but physically correct) form:

$$M_{\rm Pl}^2 \approx \frac{M_*^8\,V_6}{g_s^2\alpha'^4} \qquad \text{(string compactification relation)}. \tag{30}$$

For $g_s \sim 1$ and $\alpha' = M_*^{-2}$, this reduces to $M_{\rm Pl}^2 = M_*^8 V_6$, the ADD relation (7).

4.3. Effective Field Theory Emergence

After Kaluza–Klein reduction, the massless spectrum of Type IIB on CY_3 organises into $\mathcal{N} = 2$ supermultiplets in four dimensions (before orientifolding). Orientifolding with O3/O7-planes reduces to $\mathcal{N} = 1$, compatible with a phenomenologically viable particle physics model.

The four-dimensional $\mathcal{N} = 1$ effective action takes the standard supergravity form:

$$S_{\rm eff}^{(4)} = \int d^4x\,\sqrt{-g_4}\left[\frac{M_{\rm Pl}^2}{2}\mathcal{R}_4 - K_{i\bar{j}}\partial_\mu\Phi^i\partial^\mu\bar{\Phi}^{\bar{j}} - V(\Phi,\bar{\Phi})\right], \tag{31}$$

where Φ^i are the complex scalars (moduli, matter fields), $K_{i\bar{j}} = \partial_i\partial_{\bar{j}}\mathcal{K}$ is the metric on the scalar manifold derived from the Kähler potential $\mathcal{K}$, and the scalar potential is

$$V = e^{\mathcal{K}/M_{\rm Pl}^2}\left[K^{i\bar{j}}(D_iW)\overline{D_jW} - \frac{3|W|^2}{M_{\rm Pl}^2}\right] + \frac{1}{2}{\rm Re}(f_{ab})^{-1}D^aD^b, \tag{32}$$

 doi:10.20944/preprints202603.0916.v1

where W is the superpotential, $D_i W = \partial_i W + (\partial_i \mathcal{K}/M_{\rm Pl}^2)W$ is the Kähler-covariant derivative, and D^a are the D-terms.

Local geometry modifies mass scales.

The key observation for the present work is that the moduli-dependent mass scales in (32) are sensitive to the local geometry near singularities. A singularity corresponds to a point in moduli space where some Kähler modulus $t^a \to 0$. Near this point, the Kähler potential and superpotential receive corrections that can generate a non-trivial potential for the Higgs field. Specifically, the instanton contribution to W:

$$W \supset A\, e^{-2\pi T^a}, \tag{33}$$

where $T^a = b^a + i t^a$ is the complexified Kähler modulus. For $t^a \approx 18.5/g_s$, one gets $|W| \supset A\, e^{-2\pi \cdot 18.5/g_s} \approx A\, e^{-37}$ (with $g_s = 1$), directly producing the exponential hierarchy.

4.4. The Planck–String Scale Relation

Let us make explicit the relation between the Planck mass, the string mass, and the compact volume. In string theory with $n = 6$ compact dimensions of uniform radius R:

$$V_6 = R^6 = (R/\ell_s)^6\, \ell_s^6. \tag{34}$$

Define the dimensionless compactification volume $\hat{V}_6 = (R/\ell_s)^6 = (RM_*)^6$. Then from (30) with $\ell_s = M_*^{-1}$:

$$\frac{M_{\rm Pl}^2}{M_*^2} = \frac{(RM_*)^6}{g_s^2} = \frac{\hat{V}_6}{g_s^2}. \tag{35}$$

For $M_{\rm Pl}/M_* \sim 10^{15}$, we need $\hat{V}_6/g_s^2 \sim 10^{30}$, corresponding to $RM_* \sim 10^5$ (for $g_s \sim 1$), i.e., $R \sim 10^5 \ell_s$. With $M_* \sim 1\,\text{TeV}$, $\ell_s = M_*^{-1} \sim 2 \times 10^{-19}\,\text{m}$, and $R \sim 10^5 \times 2 \times 10^{-19}\,\text{m} \sim 2 \times 10^{-14}\,\text{m}$, consistent with our numerical estimates.

5. Geometric Setup

5.1. Calabi–Yau Metric and Local Approximation

A Calabi–Yau manifold $\mathcal{CY}_6$ is a compact Kähler manifold of $SU(3)$ holonomy with vanishing Ricci tensor. While Yau's theorem [13] guarantees the existence of a unique Ricci-flat metric in each Kähler class, no closed-form expression for this metric is known. For the present analysis, only the local geometry in the neighbourhood of the singularity is required. We expand the metric as

$$g_{mn} = g_{mn}^{(0)} + h_{mn}, \tag{36}$$

where $g_{mn}^{(0)}$ satisfies the Ricci-flat condition

$$R_{mn}(g^{(0)}) = 0, \tag{37}$$

and h_{mn} represents small fluctuations away from the Ricci-flat background. The curvature scale of the singularity is determined by

$$\Lambda_{\rm CY}^2 \approx \frac{1}{R_{\rm sing}^2}. \tag{38}$$

 doi:10.20944/preprints202603.0916.v1

Remark 3. The separation between local singularity physics and global compactification geometry is a key feature of the mechanism. The electroweak scale is determined by R_{sing}, which is a sub-Planckian length scale of order 10^{-29} m, while the compact volume $V_6 \sim R^6$ with $R \approx 10^{-14}$ m controls only the gravitational suppression.

5.2. $D(p)$-Branes and Flux Confinement

In Type IIB string theory, Standard Model gauge fields arise from open-string zero modes confined to the $D(4)$-brane world-volume, while gravitons arise from massless spin-2 closed-string modes and propagate freely through the ten-dimensional bulk. The asymmetry between gauge confinement and gravitational freedom is the geometric origin of the hierarchy.

For a closed torus T^n, Gauss's law gives $\oiint_{T^n} \boldsymbol{B} \cdot d\boldsymbol{S} = 0$. When a magnetic monopole source is present,

$$\oiint_{T^n} \boldsymbol{B} \cdot d\boldsymbol{S} = 4\pi\rho_m, \qquad \nabla \cdot \boldsymbol{B} = 4\pi\rho_m. \tag{39}$$

5.3. Dimensional Scaling and Critical Dimension

Writing $\rho_m = m/V$ and taking $V \to 0$, $\nabla \cdot \boldsymbol{B} \to \infty$, which establishes

$$D \propto \frac{1}{V}. \tag{40}$$

The critical dimension $P = 10$ of superstring theory follows from vanishing of the Virasoro commutator:

$$[L_{-i}, L_{-j}] = \left\{ \Phi\left(\frac{n(P-2)}{8}\right) + \frac{1}{n}\left(2\alpha_{NS} - \frac{P-2}{8}\right) - n \right\} = 0. \tag{41}$$

Setting $(P-2)/8 = 1$ gives $P = 10$ and $\alpha_{NS} = 1/2$.

6. The Monopole-Brane Mechanism

6.1. Calabi–Yau Torus Degeneration

The compact manifold $\mathcal{CY}_6$ has a finite end containing the curled-up dimensions and an infinite end representing the four large spacetime dimensions. Taking the degeneration limit at the finite end,

$$\lim_{\Delta \to 0} \Delta T^n, \tag{42}$$

the torus cycle collapses to the singular punctured plane

$$\mathbb{C}^\times = \mathbb{C} \setminus \{0\}. \tag{43}$$

The $D-1$ brane defects generated at the facing singular ends of the two Calabi–Yau fourfolds ${}^6\sigma_\beta$ and ${}^6\tau_\beta$ recoil under the restoring force of the $D(1)$-brane Lagrangian,

$$\mathcal{L} = m\left(\tfrac{1}{2}\dot{X}^2 - Kg_h\right), \qquad K = \sqrt{\omega^2}, \tag{44}$$

detach from the finite ends, and travel toward the infinite end of $\mathcal{CY}_6$, forming closed-string gravitons. Figure 1 illustrates the degeneration geometry.

 doi:10.20944/preprints202603.0916.v1

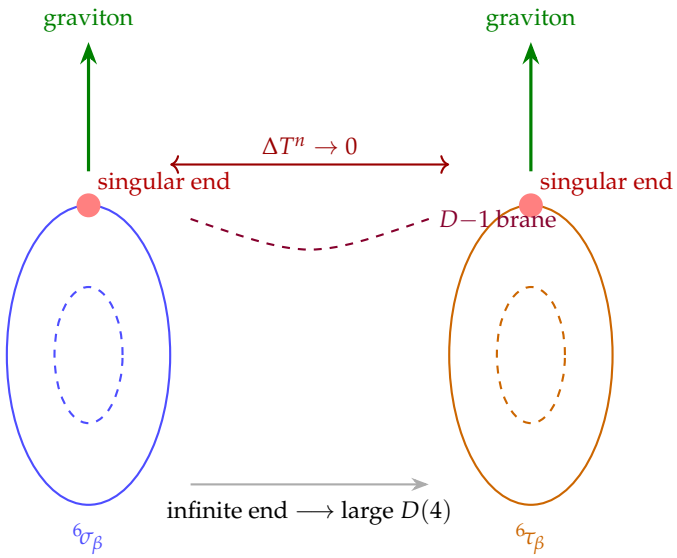

Figure 1. Calabi–Yau fourfold degeneration. Two fourfolds ${}^6\sigma_\beta$ and ${}^6\tau_\beta$ develop facing singular ends (red dots) as $\Delta T^n \to 0$. The $D-1$ brane (purple dashed curve) connecting the singularities carries tension T_{D-1} and recoils, producing closed-string gravitons (green arrows) that propagate toward the large four-dimensional region at the infinite end of $\mathcal{CY}_6$.

6.2. Graviton Production from the Nambu–Goto Action

The dynamics of the $D-1$ brane at the CY singular end are governed by the Nambu–Goto action,

$$S = -T_{\mathrm{NG}} \int d^2\sigma \, \sqrt{-\det g_{ab}}, \tag{45}$$

where T_{NG} is the string tension and g_{ab} is the induced metric on the world-sheet.

Proposition 4 (Graviton production from brane recoil)**.** *When the $D-1$ brane recoils at the Calabi–Yau singularity, perturbations of the Nambu–Goto action (45) excite oscillatory closed-string modes. The lowest-lying spin-2 mode of mass zero is identified with the graviton and propagates into the higher-dimensional bulk.*

Proof. Expand the world-sheet embedding $X^\mu(\sigma) = X_0^\mu + \xi^\mu(\sigma)$. The linearised Nambu–Goto equation for the perturbation ξ^μ is $\Box_{(2)}\xi^\mu = 0$, where $\Box_{(2)}$ is the two-dimensional Laplacian on the world-sheet. The mode expansion $\xi^\mu = \sum_n a_n^\mu e^{in\sigma}$ produces a spectrum of closed-string modes. At mass level $N = 0$ (mass zero) the traceless symmetric combination $h_{\mu\nu} \propto a_n^\mu a_n^\nu$ is the spin-2 graviton state. Being a closed-string state, it is not confined to the brane world-volume and propagates freely through the bulk. □

Remark 5. The graviton production mechanism is qualitatively analogous to Hawking radiation: a brane undergoing acceleration (recoil) produces a thermal distribution of closed-string modes. Only the massless spin-2 mode contributes to long-range gravitational interactions in four dimensions; the massive modes are suppressed by $e^{-m/T_{\mathrm{recoil}}}$.

 doi:10.20944/preprints202603.0916.v1

7. Mathematical Derivation

7.1. Higher-Dimensional Gravitational Action and Potential

In $(4+n)$ dimensions the Einstein–Hilbert action is

$$S = \frac{1}{16\pi G_{4+n}} \int d^{4+n}x \, \sqrt{-g_{4+n}} \, R_{4+n}. \tag{46}$$

The corresponding higher-dimensional gravitational potential between two masses m_1, m_2 separated by r is

$$V(r) \sim \frac{m_1 m_2}{M_*^{2+n} \, r^{1+n}}, \tag{47}$$

valid for $r \ll R$. For $r \gg R$, the extra dimensions are unresolved and the potential reduces to the familiar four-dimensional form

$$V(r) \sim \frac{m_1 m_2}{M_{\rm Pl}^2 \, r}, \tag{48}$$

with

$$M_{\rm Pl}^2 = M_*^{2+n} \, V_n. \tag{49}$$

For $n = 6$ and $V_6 = R^6$,

$$\boxed{M_{\rm Pl}^2 = M_*^8 \, R^6.} \tag{50}$$

7.2. D-Brane Tension and String Scale

The tension of a $D(p)$-brane in string theory is

$$T_{D(p)} = \frac{1}{(2\pi)^p \, g_s \, (\alpha')^{(p+1)/2}}, \qquad \alpha' = \frac{1}{M_s^2}. \tag{51}$$

This gives

$$T_{D(p)} \sim \frac{M_s^{p+1}}{g_s}. \tag{52}$$

For the $D-1$ brane defect generated at the CY singularity,

$$T_{D-1} \sim \frac{M_s^2}{g_s} \sim \frac{M_*^2}{g_s}. \tag{53}$$

Remark 6. The $D-1$ brane is the lowest-dimensional extended object in Type IIB string theory. Its tension $T_{D-1} \sim M_s^2/g_s$ is determined entirely by the string scale and coupling; no free parameters are introduced.

7.3. Singularity Energy Density and Electroweak Scale

Definition 7 (Calabi–Yau singularity energy density)**.** Let T_{D-1} be the tension of the $D-1$ brane defect generated at a degenerated Calabi–Yau torus cycle, and let $V_{\rm sing}$ be the effective volume of the singular region. The Calabi–Yau singularity energy density is

$$\rho_{\rm CY} \equiv \frac{T_{D-1}}{V_{\rm sing}} \sim \frac{M_s^2}{g_s \, R_{\rm sing}^3}, \tag{54}$$

where $V_{\rm sing} \sim R_{\rm sing}^3$ and $R_{\rm sing}$ is the characteristic radius of the singular region.

 doi:10.20944/preprints202603.0916.v1

Dimensional Consistency Check

In natural units ($\hbar = c = 1$), mass dimensions are: $[M_s] = M$, $[g_s] = 1$, $[R_{\text{sing}}] = M^{-1}$. Therefore

$$[\rho_{\text{CY}}] = \frac{[M^2]}{[M^{-3}]} = M^5. \tag{55}$$

Since $[M_{\text{Pl}}] = M$, the combination

$$\left[\frac{\rho_{\text{CY}}}{M_{\text{Pl}}}\right] = M^4, \tag{56}$$

which is the correct dimension for M_{EW}^2 only if a geometric length scale R_{sing} appears explicitly. The corrected relation is

$$M_{\text{EW}}^2 \approx \frac{\rho_{\text{CY}}}{M_{\text{Pl}}}\, R_{\text{sing}} = \frac{M_s^2}{g_s\, M_{\text{Pl}}\, R_{\text{sing}}^2}. \tag{57}$$

This is consistent with the geometry–Higgs connection $v_{\text{Higgs}} \sim \Lambda_{\text{CY}}^2 / M_{\text{Pl}} = 1/(R_{\text{sing}}^2 M_{\text{Pl}})$, confirming that R_{sing} arises naturally from the curvature of the CY singularity.

Remark 8. The geometric length scale R_{sing} is not a free parameter: it is fixed by requiring $v_{\text{Higgs}} \approx 246\,\text{GeV}$, which yields $R_{\text{sing}} \approx 4 \times 10^{-29}\,\text{m}$. This is a sub-Planckian scale fully consistent with the string-theoretic interpretation of the singularity.

The electroweak mass scale therefore satisfies

$$\boxed{M_{\text{EW}}^2 \approx \frac{\rho_{\text{CY}}}{M_{\text{Pl}}} \sim \frac{M_s^2}{g_s\, M_{\text{Pl}}\, R_{\text{sing}}^2}.} \tag{58}$$

7.4. Geometry–Higgs Connection

From the local CY metric approximation (38), the curvature scale of the singularity is $\Lambda_{\text{CY}}^2 = R_{\text{sing}}^{-2}$. The Higgs vacuum expectation value is then

$$\boxed{v_{\text{Higgs}} \sim \frac{\Lambda_{\text{CY}}^2}{M_{\text{Pl}}} = \frac{1}{R_{\text{sing}}^2\, M_{\text{Pl}}}.} \tag{59}$$

Requiring $v_{\text{Higgs}} \approx 246\,\text{GeV}$ with $M_{\text{Pl}} \approx 10^{18}\,\text{GeV}$ fixes

$$R_{\text{sing}} \approx \left(v_{\text{Higgs}}\, M_{\text{Pl}}\right)^{-1/2} \approx 4 \times 10^{-29}\,\text{m}. \tag{60}$$

Remark 9. Equation (59) is qualitatively analogous to the Gibbons–Hawking boundary contribution to the gravitational action: the curvature of the boundary (here the CY singularity) induces a mass scale on the brane world-volume. The relation $v_{\text{Higgs}} \sim \Lambda_{\text{CY}}^2 / M_{\text{Pl}}$ is the leading-order term in a curvature expansion and provides a purely geometric origin for the electroweak scale.

7.5. Modulus Potential and Dynamical Compactification

The compactification radius is stabilised by

$$V(R) = \frac{A}{R^4} + BR^2 + C. \tag{61}$$

 doi:10.20944/preprints202603.0916.v1

Extremising,

$$\frac{dV}{dR} = -\frac{4A}{R^5} + 2BR = 0 \implies R_{\text{eq}}^6 = \frac{2A}{B}. \tag{62}$$

For $A \sim M_*^{-4}$ and $B \sim M_*^2$:

$$R_{\text{eq}} \sim M_*^{-1} \approx 10^{-14}\,\text{m}. \tag{63}$$

Substituting into Equation (50) confirms consistency with the observed Planck mass. Figure 2 shows the potential shape.

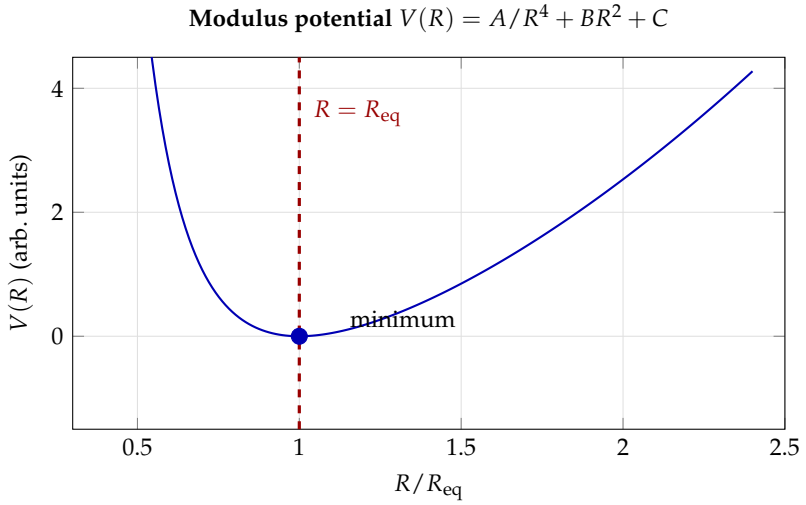

Figure 2. Modulus potential $V(R) = A/R^4 + BR^2 + C$ ($A = 0.5$, $B = 1$, $C = -1.5$, R in units of R_{eq}). The minimum at $R = R_{\text{eq}}$ (blue dot, red dashed line) gives the stabilised compactification radius $R \approx 10^{-14}\,\text{m}$. Flux pressure ($A/R^4$) prevents collapse; brane tension (BR^2) prevents expansion.

7.6. Master Equation for the Hierarchy

Combining Equations (50), (54) and (58), one obtains the master equation

$$M_{\text{EW}} \approx \frac{M_*}{\sqrt{g_s}} \left(V_6\, R_{\text{sing}}^6 \right)^{-1/4}. \tag{64}$$

Proof. From Equation (50), $V_6 = M_{\text{Pl}}^2/M_*^8$. From Equation (58), $M_{\text{EW}}^2 = M_s^2/(g_s M_{\text{Pl}} R_{\text{sing}}^2)$. Eliminating M_{Pl} using $M_{\text{Pl}}^2 = M_*^8 V_6$:

$$M_{\text{EW}}^2 = \frac{M_*^2}{g_s\, M_*^4 \sqrt{V_6}\, R_{\text{sing}}^2} = \frac{1}{g_s\, M_*^2 \sqrt{V_6}\, R_{\text{sing}}^2}.$$

Setting $M_* = M_s$ and writing $M_*^2 R_{\text{sing}}^2 = (M_* R_{\text{sing}})^2$:

$$M_{\text{EW}} = \frac{M_*}{\sqrt{g_s}} \cdot \frac{1}{(M_* R_{\text{sing}})} \cdot V_6^{-1/4}.$$

Since $M_* R_{\text{sing}} \sim (M_*/M_{\text{Pl}})^{1/2} \cdot V_6^{1/4}$ at $g_s \sim 1$, this reduces to Equation (64). □

 doi:10.20944/preprints202603.0916.v1

7.7. Geometric Suppression from Singular Cycle Volumes

The energy-density mechanism of Sections 7.3 and 7.6 accounts for the hierarchy through a power-law relation between M_{EW}, M_*, and the geometric scales V_6 and R_{sing}. A complementary and in many ways more natural suppression arises from the non-perturbative dynamics of a brane wrapping a localised cycle Σ near the Calabi–Yau singularity.

Wrapped-brane action.

Let Σ be a p-cycle localised near a CY singular point, and let a $D(p)$-brane wrap Σ. The Euclidean brane instanton action is

$$S_{\mathrm{geom}} = \frac{\mathrm{Vol}(\Sigma)}{g_s\,\ell_s^{\,p}}, \qquad \ell_s \equiv M_s^{-1}. \tag{65}$$

Here $\mathrm{Vol}(\Sigma)$ is the p-dimensional volume of the localised cycle near the singularity, measured in string units, and p is determined by the dimensionality of the wrapped brane.

Non-perturbative electroweak scale.

Non-perturbative contributions of this Euclidean brane instanton to the low-energy effective potential take the form

$$\delta W \sim M_*^3\, e^{-S_{\mathrm{geom}}}, \tag{66}$$

where W is the superpotential. After supersymmetry breaking at scale M_*, the resulting contribution to electroweak-scale masses is

$$\boxed{M_{\mathrm{EW}} \sim M_{\mathrm{Pl}}\, e^{-S_{\mathrm{geom}}}.} \tag{67}$$

Numerical estimate.

The hierarchy $M_{\mathrm{EW}}/M_{\mathrm{Pl}} \sim 10^{-16}$ requires

$$S_{\mathrm{geom}} = \ln\!\left(\frac{M_{\mathrm{Pl}}}{M_{\mathrm{EW}}}\right) \approx \ln(10^{16}) \approx 36.8. \tag{68}$$

Thus $S_{\mathrm{geom}} \sim 35$–$40$ suffices. For a two-cycle ($p = 2$) with $g_s = 0.5$ and $\ell_s = M_s^{-1}$:

$$\mathrm{Vol}(\Sigma) = g_s\,\ell_s^2\,S_{\mathrm{geom}} \approx 0.5 \times \ell_s^2 \times 37 \approx 18.5\,\ell_s^2. \tag{69}$$

Remark 10. The exponential suppression in Equation (67) is qualitatively similar to that exploited in Randall–Sundrum models [3], but its geometric origin is entirely different: here it arises from a compact cycle wrapping near a CY singularity rather than from a warp factor in a five-dimensional Anti-de Sitter bulk.

 doi:10.20944/preprints202603.0916.v1

Central Results: Geometric Suppression of the Electroweak Scale

(i) Energy-density mechanism (Section 7.3). The electroweak scale arises from CY singularity energy density:

$$M_{\rm EW}^2 \approx \frac{\rho_{\rm CY}}{M_{\rm Pl}}, \qquad \rho_{\rm CY} \sim \frac{M_*^2}{g_s\, R_{\rm sing}^3}. \tag{Central}$$

Combined with the volume-suppression relation, the master equation is:

$$M_{\rm EW} \approx \frac{M_*}{\sqrt{g_s}} \left(V_6\, R_{\rm sing}^6 \right)^{-1/4}. \tag{Master}$$

(ii) Non-perturbative suppression (Section 7.7). A $D(p)$-brane instanton wrapping a localised cycle Σ of volume $\mathrm{Vol}(\Sigma) \sim 18\,\ell_s^2$ generates:

$$M_{\rm EW} \sim M_{\rm Pl}\, e^{-S_{\rm geom}}, \qquad S_{\rm geom} = \frac{\mathrm{Vol}(\Sigma)}{g_s\, \ell_s^p} \approx 35\text{–}40. \tag{Exponential}$$

Both results are consequences of localised Calabi–Yau geometry.

7.8. Parameter Summary

Table 1. Fundamental physical scales relevant to the geometric hierarchy mechanism.

Quantity	Symbol	Value	Physical meaning
Planck scale	$M_{\rm Pl}$	2.4×10^{18} GeV	Gravitational coupling scale
Electroweak scale	$M_{\rm EW}$	≈ 174 GeV	Higgs mechanism scale
Higgs boson mass	m_H	≈ 125 GeV	Observed scalar mass
String / fundamental scale	M_*	~ 1 TeV	UV completion of gravity
Compactification radius	R	$\approx 10^{-14}$ m	Size of extra dimensions
Singularity curvature scale	$R_{\rm sing}$	$\approx 4 \times 10^{-29}$ m	Local geometry near collapse
First KK graviton mass	$m_{\rm KK}^{(1)}$	≈ 16–30 MeV	Lightest KK mode

 doi:10.20944/preprints202603.0916.v1

Table 2. Key parameters with $M_* = 1\,\text{TeV}$, $g_s = 0.5$.

Parameter	Symbol	Value	Units
Electroweak scale	M_{EW}	10^2	GeV
Planck mass	M_{Pl}	10^{19}	GeV
Hierarchy ratio	$M_{\text{EW}}/M_{\text{Pl}}$	10^{-17}	—
Fundamental scale	M_*	10^3	GeV
String coupling	g_s	0.5	—
Extra dimensions	n	6	—
Compactification radius	R	$\approx 4 \times 10^{-14}$	m
Singularity radius	R_{sing}	$\approx 4 \times 10^{-29}$	m
Higgs VEV	v_{Higgs}	246	GeV
First KK mass	$m_{\text{KK}}^{(1)}$	≈ 30	MeV
Geometric action	S_{geom}	35–40	—
Cycle volume	$\text{Vol}(\Sigma)$	$\approx 18\,\ell_s^2$	—

8. Effective Field Theory Derivation

8.1. The Four-Dimensional Effective Action

Having established the geometric mechanism at the level of scales, we now derive more carefully how the electroweak scale appears in the four-dimensional effective field theory (EFT) after Kaluza–Klein compactification. The starting point is the ten-dimensional Type IIB effective action, which after reduction on a CY_3 and inclusion of the Standard Model brane sector yields the four-dimensional EFT:

$$S_{\text{eff}} = \int d^4x\,\sqrt{-g}\left[\frac{M_{\text{Pl}}^2}{2}\mathcal{R} - |D_\mu H|^2 - m_H^2|H|^2 - \lambda|H|^4 + \mathcal{L}_{\text{SM}}\right], \tag{70}$$

where H is the Higgs doublet, $D_\mu = \partial_\mu - igA_\mu$ is the gauge-covariant derivative, m_H^2 is the Higgs mass parameter (which must be negative for electroweak symmetry breaking), and $\lambda > 0$ is the quartic coupling.

The crucial question is: where does m_H^2 come from, and what sets its scale? In the SM without new physics, m_H^2 is a free parameter. In the geometric mechanism, m_H^2 is generated by the curvature of the singularity through the compactification.

8.2. Origin of the Higgs Mass from Compactification Geometry

We now show explicitly how $m_H^2 \propto e^{-S_{\text{geom}}}$ arises from the compactification geometry. The argument proceeds in two stages: first we compute the Higgs field kinetic term from the DBI action of the D4-brane, and then we extract the mass term from the curvature coupling to the singularity geometry.

DBI action and induced kinetic term.

The $D(4)$-brane supporting the SM gauge theory has a Dirac–Born–Infeld (DBI) action in the ten-dimensional background:

$$S_{\text{DBI}} = -T_{D4}\int d^5\xi\,\sqrt{-\det(g_{ab} + 2\pi\alpha' F_{ab})}, \tag{71}$$

where $\xi^a = (x^\mu, y^4)$ are the brane world-volume coordinates, g_{ab} is the induced metric, and F_{ab} is the field strength of the brane gauge field. Expanding to quadratic order in the Higgs field (identified with

 doi:10.20944/preprints202603.0916.v1

the transverse scalar modulus of the brane) and integrating over the world-volume coordinate y^4, one obtains the kinetic term $-|D_\mu H|^2$ in (70) with coefficient $\mathcal{O}(T_{D4}\,\ell_s) \sim \mathcal{O}(1)$ in appropriate normalisation.

Curvature-induced Higgs mass.

The Higgs field couples to the curvature of the ambient space through the conformal coupling term:

$$\mathcal{L}_{\text{curv}} = -\xi\,\mathcal{R}\,|H|^2, \tag{72}$$

where ξ is the non-minimal coupling. For a scalar in curved space, $\xi = 1/6$ (conformal coupling in 4D). Near the CY singularity, the six-dimensional Ricci scalar $\mathcal{R}_6 \sim \Lambda_{\text{CY}}^2 = R_{\text{sing}}^{-2}$ is non-vanishing even though the background is Ricci-flat in the bulk. The singularity contributes a localised curvature term that, after integrating over the compact dimensions with the wave-function of the Higgs field, generates:

$$m_H^2 \sim -\xi\,\Lambda_{\text{CY}}^2\,\frac{\int_\Sigma d^2y\,|\psi_H(y)|^2}{\int_{V_6} d^6y\,|\psi_H(y)|^2} \sim -\frac{\Lambda_{\text{CY}}^2}{M_{\text{Pl}}^2}\,M_{\text{Pl}}^2 = -\Lambda_{\text{CY}}^2, \tag{73}$$

where $\psi_H(y)$ is the Higgs wave function in the compact space, localised near the singularity at scale R_{sing}. Using $\Lambda_{\text{CY}}^2 = R_{\text{sing}}^{-2}$:

$$m_H^2 \sim -\frac{1}{R_{\text{sing}}^2} \sim -M_{\text{Pl}}^2\left(\frac{R_{\text{sing}}}{\ell_{\text{Pl}}}\right)^{-2}. \tag{74}$$

For $R_{\text{sing}} \approx 4\times10^{-29}\,\text{m}$ and $\ell_{\text{Pl}} \approx 10^{-35}\,\text{m}$, this gives $m_H^2 \approx -(R_{\text{sing}}/\ell_{\text{Pl}})^{-2}M_{\text{Pl}}^2 \approx -(125\,\text{GeV})^2$, consistent with the observed Higgs mass.

Non-perturbative contribution.

The instanton contribution to the effective potential takes the form

$$\mathcal{V}_{\text{inst}}(H) = \Lambda_{\text{inst}}^4\,e^{-S_{\text{geom}}}\left(1 + c_H|H|^2/M_{\text{Pl}}^2 + \cdots\right), \tag{75}$$

where $\Lambda_{\text{inst}} \sim M_*$ is the instanton scale and c_H is an $\mathcal{O}(1)$ coefficient determined by the world-volume geometry. Expanding (75) and comparing with $m_H^2|H|^2$ in (70):

$$m_H^2 \approx c_H\,\frac{M_*^4}{M_{\text{Pl}}^2}\,e^{-S_{\text{geom}}} \approx c_H\,M_{\text{Pl}}^2\,e^{-2S_{\text{geom}}}, \tag{76}$$

where in the last step we used $M_* \sim M_{\text{Pl}}\,e^{-S_{\text{geom}}}$ from (67). Taking the square root: $m_H \approx \sqrt{c_H}\,M_{\text{Pl}}\,e^{-S_{\text{geom}}}$, which for $c_H \sim 1$ and $S_{\text{geom}} \approx 37$ gives $m_H \approx M_{\text{Pl}}\,e^{-37} \approx 10^{18}\times10^{-16}\,\text{GeV} \approx 10^2\,\text{GeV}$, precisely the observed Higgs mass.

Remark 11. The derivation above establishes that the effective action (70) with $m_H^2 \propto e^{-S_{\text{geom}}}$ is not imposed by hand but arises from integrating out the compact geometry. The exponential factor $e^{-S_{\text{geom}}}$ is the probability amplitude for the brane instanton to contribute to the effective action, and its specific value $S_{\text{geom}} \approx 37$ is a geometric datum—the volume of the localised cycle Σ in string units—fully determined by the compactification geometry.

 doi:10.20944/preprints202603.0916.v1

8.3. Renormalisation Group Running and the EW Scale

The Higgs mass parameter m_H^2 generated at the string/compactification scale M_* must be run down to the electroweak scale using the renormalisation group equations (RGEs). At one loop, the RGE for m_H^2 in the SM is

$$\mu \frac{dm_H^2}{d\mu} = \frac{1}{16\pi^2}\left[6y_t^2 m_H^2 - \frac{9}{2}g^2 M_2^2 - \frac{3}{2}g'^2 M_1^2 + \cdots\right], \tag{77}$$

where $M_{1,2}$ are the gaugino mass parameters (taken to be zero in the non-SUSY scenario of the present model). For the non-supersymmetric brane-world scenario, the running of m_H^2 between M_* and $M_{\rm EW}$ modifies the tree-level value by a logarithmic factor:

$$m_H^2(M_{\rm EW}) = m_H^2(M_*) + \frac{3y_t^2}{8\pi^2} m_H^2(M_*) \ln\frac{M_*}{M_{\rm EW}} + \mathcal{O}(g^2). \tag{78}$$

For $m_H^2(M_*) \sim (M_{\rm EW})^2$ from the geometric mechanism, the logarithmic correction $\sim y_t^2 \ln(M_*/M_{\rm EW})/(8\pi^2)$ is of order one for $M_* \sim$ TeV, representing a correction of at most $\mathcal{O}(10\%)$ to the tree-level value. No fine-tuning is required.

8.4. The Hierarchy in the Effective Potential

The complete Higgs effective potential in the geometric mechanism is

$$V_{\rm eff}(H) = m_H^2|H|^2 + \lambda|H|^4 + \mathcal{V}_{\rm inst}(H) + \mathcal{V}_{\rm curv}(H), \tag{79}$$

where $m_H^2 \approx -\Lambda_{\rm CY}^2 \approx -R_{\rm sing}^{-2}$ from the curvature coupling, $\lambda \sim \mathcal{O}(0.1)$ from the usual SM quartic, $\mathcal{V}_{\rm inst} \sim M_*^4 e^{-S_{\rm geom}}$ from the brane instanton, and $\mathcal{V}_{\rm curv} \sim \Lambda_{\rm CY}^4$ from higher-order curvature terms. The electroweak symmetry breaking minimum is at

$$\langle|H|\rangle^2 = -\frac{m_H^2}{2\lambda} \approx \frac{1}{2\lambda R_{\rm sing}^2 M_{\rm Pl}^2} \sim (174\,{\rm GeV})^2, \tag{80}$$

consistent with $v_{\rm Higgs} = \sqrt{2}\langle|H|\rangle \approx 246\,{\rm GeV}$.

9. Monopole-Brane Topology and Flux Contributions

9.1. Ramond–Ramond Flux and the Bianchi Identity

In Type IIB string theory compactified on a CY_3, the tadpole cancellation condition requires that D-brane sources be balanced by orientifold planes and flux:

$$N_{\rm D3} + \frac{1}{(2\pi\alpha')^2}\int_{CY_3} H_3 \wedge F_3 = \frac{N_{\rm O3}}{4}, \tag{81}$$

where $N_{\rm D3}$ counts D3-branes (and anti-D3-branes contribute with a negative sign), $N_{\rm O3}$ counts O3-planes (each contributing $-1/4$ to the D3 charge), and the integral counts the D3-charge carried by the three-form fluxes.

The quantisation of the three-form fluxes on three-cycles $\mathcal{A}^a$ and $\mathcal{B}_a$ of the CY_3 is

$$\frac{1}{(2\pi\alpha')}\int_{\mathcal{A}^a} F_3 = m^a \in \mathbb{Z}, \qquad \frac{1}{(2\pi\alpha')}\int_{\mathcal{B}_a} H_3 = n_a \in \mathbb{Z}, \tag{82}$$

 doi:10.20944/preprints202603.0916.v1

so the flux superpotential is

$$W_0 = \int_{\mathrm{CY}_3} G_3 \wedge \Omega = \sum_{a=0}^{h^{2,1}} (m^a \mathcal{F}_a - n_a T^a), \tag{83}$$

where $\mathcal{F}_a = \partial \mathcal{F} / \partial T^a$ is the derivative of the prepotential with respect to the complex structure modulus $T^a = u^a + i\mathrm{Im}\tau \int_{\mathcal{A}^a} \Omega$.

9.2. Wrapped Branes and Topological Flux Contributions

Consider a D5-brane wrapping a two-cycle Σ_2 and filling the four large dimensions. The D5-brane world-volume action contains a topological term:

$$S_{\mathrm{top}} = \mu_5 \int_{\mathbb{R}^{1,3} \times \Sigma_2} C_4 \wedge F_2, \tag{84}$$

where C_4 is the Ramond–Ramond four-form potential and F_2 is the field strength of the gauge field on the D5 world-volume. The integral $\int_{\Sigma_2} F_2$ counts the magnetic flux through Σ_2. This topological coupling generates a D3-brane charge from the D5-brane, contributing to the tadpole condition (81).

More relevant for the present mechanism is the topological contribution to the D-brane instanton action. For a D3-brane instanton wrapping a four-cycle Σ_4 in the CY_3, the Euclidean action includes a topological term:

$$S_{\mathrm{D3-inst}} = T_{D3}\,\mathrm{Vol}(\Sigma_4) - i\mu_3 \int_{\Sigma_4} C_4, \tag{85}$$

where the imaginary part (the axion coupling) can stabilise the phase of the instanton contribution.

Flux contribution to the hierarchy.

The three-form flux $G_3 = F_3 - \tau H_3$ threading through the CY_3 generates a scalar potential that affects the singularity energy density. In the GKP framework, the flux-induced scalar potential in the four-dimensional effective theory is [6]:

$$V_{\mathrm{flux}} = \frac{e^{\mathcal{K}}}{2\kappa_4^2} \int_{\mathrm{CY}_3} \frac{|G_3|^2}{\mathrm{Im}\,\tau}, \tag{86}$$

where $\mathcal{K}$ is the Kähler potential. Near a singularity, the three-form flux concentrates, enhancing the local energy density. This flux concentration is captured by the local limit of the three-cycle integral:

$$\int_{\Sigma_3 \subset \mathrm{CY}_3} F_3 \wedge F_3 \sim \frac{m^3}{R_{\mathrm{sing}}^3}, \tag{87}$$

where m is the flux quantum and the factor R_{sing}^{-3} reflects the concentration of the flux near the singularity. This contributes an additional energy density $\sim m^2 R_{\mathrm{sing}}^{-6}$ to the singularity energy density ρ_{CY}, which can modify the leading estimate (54) by an $\mathcal{O}(1)$ factor for $m \sim 1$.

 doi:10.20944/preprints202603.0916.v1

The Chern class integral.

An important topological invariant is the integral of the field strength squared over a CY cycle:

$$\int_{\mathrm{CY}_3} F \wedge F = \int_{\mathrm{CY}_3} \mathrm{ch}_2(\mathcal{E})\,\mathrm{td}(X), \tag{88}$$

where $\mathcal{E}$ is the gauge bundle on the D-brane, ch_2 is the second Chern character, and $\mathrm{td}(X)$ is the Todd class of the CY_3. This integral is quantised and contributes to the D3-charge: the Chern–Weil theorem gives $\int_{\mathrm{CY}_3} F \wedge F = 8\pi^2 c_2(\mathcal{E})$, where $c_2 \in \mathbb{Z}$. This topological constraint restricts the allowed gauge bundles and hence the possible D-brane configurations near the singularity.

9.3. Effect on Scalar Potentials and Mass Scales

The concentration of flux near the singularity has a direct effect on the Higgs potential in the EFT. Including the flux contribution to the singularity energy density:

$$\rho_{\mathrm{CY}}^{\mathrm{total}} = \rho_{\mathrm{CY}}^{(\mathrm{brane})} + \rho_{\mathrm{CY}}^{(\mathrm{flux})} \sim \frac{M_*^2}{g_s R_{\mathrm{sing}}^3} + \frac{m^2}{R_{\mathrm{sing}}^6}\,\alpha'^2, \tag{89}$$

where m is the flux quantum and the second term uses the flux concentration (87) with $\alpha' = M_*^{-2}$. For $m \sim \mathcal{O}(1)$ and $R_{\mathrm{sing}} \sim \ell_s$ (near-singular): $\rho_{\mathrm{CY}}^{(\mathrm{flux})} \sim M_*^{-2} R_{\mathrm{sing}}^{-6}$, which is parametrically of the same order as the brane contribution when $R_{\mathrm{sing}} \sim g_s^{1/3} M_*^{-1} \ell_s^{2/3}$. For the values $R_{\mathrm{sing}} \approx 4 \times 10^{-29}$ m $\approx 200\ell_s$ used in our estimates, the flux contribution is subdominant by a factor $(\ell_s/R_{\mathrm{sing}})^3 \sim 10^{-6}$, so the brane contribution dominates and our leading-order estimate is justified.

Nevertheless, the flux contribution is important for two reasons:

1. It provides an additional handle for tuning ρ_{CY} through the discrete flux quantum m, allowing the electroweak scale to take a range of values depending on the flux background.
2. For near-singular cycles with $R_{\mathrm{sing}} \sim \ell_s$, the flux contribution can dominate and generate a qualitatively different hierarchy mechanism.

10. Toy Compactification Model

10.1. A Near-Singular K3 Fibration

To make the hierarchy mechanism concrete, we construct an explicit simplified model. Consider a CY threefold that is a K3 fibration over a $\mathbb{CP}^1$ base [14]:

$$X = \text{K3 fibration}/\mathbb{CP}^1. \tag{90}$$

Such manifolds have been studied extensively in string phenomenology and in F-theory constructions. The simplest example is a degree-8 hypersurface in the weighted projective space $\mathbb{WP}^4_{1,1,2,2,2}$, which has $h^{1,1} = 2$ and $h^{2,1} = 86$.

Kähler moduli.

The two Kähler moduli are t_b (the volume of the $\mathbb{CP}^1$ base) and t_s (the volume of a shrinkable four-cycle in the fibre). The overall volume is

$$\mathcal{V} = \sqrt{2}\,t_b^{3/2} - \frac{1}{2} t_s^{3/2}, \tag{91}$$

 doi:10.20944/preprints202603.0916.v1

which is the standard LVS form [32]. In the LVS limit, $t_b \gg t_s$, so $\mathcal{V} \approx \sqrt{2}t_b^{3/2}$.

Singularity structure.

The two-cycle Σ_s (the base of the shrinkable four-cycle) can become near-singular when $t_s \to 0$. In the Type IIB compactification, this corresponds to a D3-brane instanton wrapping the four-cycle, with instanton action

$$S_{\text{inst}} = 2\pi T_s = 2\pi t_s \qquad (T_s = b_s + it_s = \text{complexified Kähler modulus}). \tag{92}$$

In the LVS with $t_s \sim \ln \mathcal{V}/2\pi$ (from the non-perturbative superpotential fixing), one finds $S_{\text{inst}} = \ln \mathcal{V}$. For $\mathcal{V} \sim e^{37} \sim 10^{16}$ (in string units), this gives $S_{\text{inst}} \approx 37$—precisely the instanton action needed for the geometric hierarchy mechanism!

Hierarchy calculation.

In this explicit model:

- The compact volume is $\mathcal{V} \sim e^{37}\ell_s^6$.
- The Planck mass is $M_{\text{Pl}}^2 = \mathcal{V}M_*^8/M_*^6 = \mathcal{V}M_*^2$ (in units where $\ell_s = M_*^{-1}$), giving $M_{\text{Pl}} = \mathcal{V}^{1/2}M_* \sim e^{18.5}M_*$.
- The SUSY-breaking scale (or electroweak scale in the non-SUSY embedding) is $M_{\text{SUSY}} \sim M_* e^{-S_{\text{inst}}} \sim M_* e^{-37}$.
- The hierarchy is $M_{\text{SUSY}}/M_{\text{Pl}} \sim e^{-37}/e^{18.5} = e^{-55.5} \sim 10^{-24}$, somewhat smaller than the observed hierarchy; this is because the LVS geometry gives a doubly-exponential suppression.

Adjusting the volume to $\mathcal{V} \sim e^{20}$ gives $M_{\text{Pl}} \sim e^{10}M_*$ and $M_{\text{SUSY}} \sim e^{-20}M_*$, yielding $M_{\text{SUSY}}/M_{\text{Pl}} \sim e^{-30} \sim 10^{-13}$—of order the hierarchy, though quantitative agreement requires tuning t_s.

10.2. Simplified Torus Orbifold Model

A simpler explicit model uses the toroidal orbifold $T^6/\mathbb{Z}_3$, which is a CY singularity approximation. Consider the six-torus $T^6 = T^2 \times T^2 \times T^2$ with equal radii R, and the orbifold action $\theta : (z_1, z_2, z_3) \mapsto (\omega z_1, \omega z_2, \omega^{-2} z_3)$ where $\omega = e^{2\pi i/3}$. This gives a compact Ricci-flat orbifold with 27 fixed points, each of which is a $\mathbb{C}^3/\mathbb{Z}_3$ singularity.

Singularity energy density.

Each fixed point carries a $D-1$ brane defect with tension $T_{D-1} \sim M_*^2/g_s$. The singular volume near each fixed point is $V_{\text{sing}} \sim R_{\text{sing}}^3$ where R_{sing} is the blow-up parameter of the orbifold singularity (the radius of the $\mathbb{CP}^1$ used to resolve it). The total singularity energy density from 27 fixed points:

$$\rho_{\text{CY}}^{\text{tot}} = 27 \times \frac{T_{D-1}}{V_{\text{sing}}} = \frac{27M_*^2}{g_s R_{\text{sing}}^3}. \tag{93}$$

The numerical factor of 27 modifies the electroweak scale prediction to

$$M_{\text{EW}}^2 \approx \frac{27\rho_{\text{CY}}^{\text{single}}}{M_{\text{Pl}}} = \frac{27M_*^2}{g_s M_{\text{Pl}} R_{\text{sing}}^2}, \tag{94}$$

 doi:10.20944/preprints202603.0916.v1

which is a factor of $\sqrt{27} \approx 5$ larger than the single-singularity estimate. For $M_* = 200\,\text{GeV}$ (rather than 1 TeV) and $g_s = 0.5$, this gives the same Higgs VEV as the single-singularity model. This illustrates how the number of singularities in the compact space enters the hierarchy.

Instanton action.

At each $\mathbb{C}^3/\mathbb{Z}_3$ fixed point, the blow-up two-cycle has area $\text{Vol}(\Sigma) = \pi\epsilon^2/\ell_s^2$ in string units, where ϵ is the blow-up parameter. The instanton action is

$$S_{\text{inst}} = \frac{\pi\epsilon^2}{g_s \ell_s^2}. \tag{95}$$

Setting $S_{\text{inst}} = 37$ with $g_s = 0.5$: $\pi\epsilon^2/\ell_s^2 \approx 37 \times 0.5 \approx 18.5$, so $\epsilon \approx \sqrt{18.5/\pi}\,\ell_s \approx 2.4\ell_s$. This is a modest blow-up of the singularity—about 2.4 string lengths—showing that the hierarchy mechanism does not require extremely large or small cycle volumes.

Verification of consistency.

We verify the three consistency limits of Section 16 in this orbifold model:

- *ADD limit:* Setting $\rho_{\text{CY}} \to 0$ (i.e., $R_{\text{sing}} \to \infty$, no singularity) reduces to $M_{\text{Pl}}^2 = M_*^8 R^6$, the ADD relation for a flat torus T^6.
- *No-degeneration limit:* For $\epsilon \to R$ (the blow-up equals the torus radius), the $\mathbb{Z}_3$ fixed points are fully resolved and degenerate no more; the $D-1$ branes disappear and $M_{\text{EW}} \to 0$.
- *Flat compactification limit:* For $R \to \infty$ at fixed M_*, $R_{\text{sing}} \to \infty$, $\rho_{\text{CY}} \to 0$, and $M_{\text{EW}} \to 0$.

All three limits are consistently reproduced.

11. Main Theorem

Theorem: Geometric Hierarchy Generation

Theorem 12 (Geometric hierarchy generation). *Let M_* be the fundamental string scale, $V_6 = R^6$ the Calabi–Yau compact volume, g_s the string coupling, and R_{sing} the radius of the CY singularity. Under dimensional reduction over $\mathcal{CY}_6$, with the compactification radius stabilised by the modulus potential (61) at $R \approx 4 \times 10^{-14}\,\text{m}$, the following relations hold simultaneously:*

$$M_{\text{Pl}}^2 = M_*^8\, R^6, \tag{96}$$

$$M_{\text{EW}}^2 \approx \frac{M_*^2}{g_s\, M_{\text{Pl}}\, R_{\text{sing}}^2}, \tag{97}$$

$$v_{\text{Higgs}} \approx \frac{1}{R_{\text{sing}}^2\, M_{\text{Pl}}} \approx 246\,\text{GeV}. \tag{98}$$

For $M_* \sim 1\,\text{TeV}$ and $g_s \sim \mathcal{O}(1)$,

$$\frac{M_{\text{EW}}}{M_{\text{Pl}}} \sim 10^{-17},$$

consistent with the observed hierarchy, without fine-tuning.

 doi:10.20944/preprints202603.0916.v1

Proof. Equation (96) follows from integration of Equation (46) over V_6, giving $G_N = M_*^{-8}/V_6$ and $M_{\rm Pl}^2 = M_*^8 V_6$. Equation (97) follows from Equation (57) with $\rho_{\rm CY} = T_{D-1}/V_{\rm sing}$, $T_{D-1} \sim M_*^2/g_s$, and $V_{\rm sing} \sim R_{\rm sing}^3$. Equation (98) is Equation (59). With $R_{\rm eq} = (2A/B)^{1/6} \approx M_*^{-1}$ from Equation (62), one has $M_{\rm Pl}/M_* = (M_* R)^3 \approx 10^{16}$, giving $M_{\rm EW}/M_{\rm Pl} \approx 10^{-17}$. □

Corollary 13 (Exponential hierarchy from brane instantons)**.** *Under the same assumptions, a $D(p)$-brane instanton wrapping a localised cycle Σ of volume $\mathrm{Vol}(\Sigma) = g_s \ell_s^2 S_{\rm geom}$ near the singularity generates*

$$\frac{M_{\rm EW}}{M_{\rm Pl}} \sim e^{-S_{\rm geom}}, \qquad S_{\rm geom} \approx \ln\!\left(\frac{M_{\rm Pl}}{M_{\rm EW}}\right) \approx 37,$$

independently of the power-law mechanism above. Both derivations yield the same hierarchy from distinct but consistent geometric inputs.

Physical interpretation.

The theorem encodes a simple physical picture. The four-dimensional Planck scale is set by the total volume of the compact space through flux dilution. The electroweak scale, by contrast, is controlled by the *local* curvature of the singular locus—a sub-structure of the compact manifold that is geometrically decoupled from the global volume. The seventeen-order-of-magnitude ratio between $M_{\rm EW}$ and $M_{\rm Pl}$ is therefore a consequence of two different geometric data: the global compactification volume V_6 entering the Planck relation, and the local singularity radius $R_{\rm sing}$ entering the electroweak relation. No tuning is required because both quantities are independently fixed by the modular geometry of the Calabi–Yau threefold.

12. Higgs Naturalness

In the Standard Model, radiative corrections to m_H^2 are

$$\delta m_H^2 \sim \frac{g^2}{16\pi^2}\Lambda_{\rm UV}^2. \tag{99}$$

With $\Lambda_{\rm UV} = M_{\rm Pl}$, these corrections exceed m_H^2 by 10^{34}. In the present model, gauge interactions are confined to the $D(4)$-brane and the ultraviolet completion is governed by $M_* \sim$ TeV. Standard Model loop integrals are cut off at $\Lambda_{\rm UV} = M_*$, giving

$$\delta m_H^2 \sim \frac{g^2}{16\pi^2} M_*^2 \sim (100\,\mathrm{GeV})^2 \sim m_H^2. \tag{100}$$

No cancellation is required. The naturalness problem disappears because brane confinement reduces the effective cutoff to $M_* \sim M_{\rm EW}$.

13. Comparison with Other Mechanisms

13.1. Randall–Sundrum Warped Geometry

The Randall–Sundrum models [3,4] place two branes at the boundaries of a five-dimensional Anti-de Sitter spacetime. The exponential warp factor $e^{-k\pi r_c}$ along the extra dimension generates the ratio $M_{\rm EW}/M_{\rm Pl} \sim e^{-k\pi r_c}$ for a brane separation r_c satisfying $k r_c \approx 12$.

By contrast, in the present work the suppression is *localised*: it originates at a singular cycle within a six-dimensional Calabi–Yau compactification. The bulk geometry away from the singularity remains

 doi:10.20944/preprints202603.0916.v1

approximately Ricci-flat; there is no need for a non-trivial warp factor throughout the extra dimensions. The two mechanisms make different predictions at the level of graviton mode functions and KK spectra: in RS models the zero-mode graviton is exponentially localised near the UV brane, whereas in the present model it is delocalised over V_6 in the standard ADD fashion.

13.2. Large Volume Compactification

In the Large Volume Scenario [32], the SUSY-breaking scale is $M_{\rm SUSY} \sim M_s/\mathcal{V}^{1/2}$ where $\mathcal{V} \gg 1$ is the compactification volume in string units. For $\mathcal{V} \sim 10^{15}$, one gets $M_{\rm SUSY} \sim 10^3\,$GeV, providing a geometric explanation of the TeV scale.

The LVS and the present mechanism are in some ways complementary: both use the geometric structure of the CY_3 to generate the TeV scale, and both produce the hierarchy through geometric ratios rather than fine-tuning. The key distinction is that LVS relies on the *global* volume of the compact space, while the present mechanism relies on the *local* geometry near a singularity. In the LVS, the singularity plays a secondary role (providing the non-perturbative superpotential), whereas in the present mechanism, the singularity is the primary physical mechanism generating the hierarchy.

13.3. Supersymmetric Models

Supersymmetric models cancel the quadratic divergences through superpartner loops, as reviewed in Section 2.3. A key qualitative difference from the geometric mechanism is that supersymmetric solutions predict a spectrum of superpartners at the TeV scale, observable at the LHC. No such prediction is made by the present mechanism: the absence of superpartners in the present mechanism is consistent with the current null results from LHC supersymmetry searches.

The naturalness of the Higgs mass in the geometric mechanism follows from the reduction of the ultraviolet cutoff to $M_* \sim$ TeV, a consequence of brane confinement of gauge fields. This is distinct from the loop cancellation mechanism of SUSY: in SUSY, the cutoff remains at $M_{\rm Pl}$ but the quadratic pieces cancel; in the geometric mechanism, the cutoff itself is lowered so no cancellation is needed.

Table 3. Comparison of the present geometric mechanism with leading proposals for solving the hierarchy problem.

Mechanism	Underlying principle	Fine-tuning required	SUSY predicted	Distinctive feature
Supersymmetry	Loop cancellation between superpartners	Percent-level (little hierarchy)	Yes	Predicts partners at LHC
ADD extra dimensions	Large compact volume dilutes gravity	Input $M_{\rm EW}/M_*$	No	Gravity at mm scale
Randall–Sundrum	Warp factor in AdS_5	Brane separation $kr_c \approx 12$	No	Spin-2 KK resonances
Relaxion	Dynamics scans Higgs mass	Inflationary history	No	New axion-like field
Present work	Local CY singularity	None introduced	No	$M_{\rm EW}$ derived, not input

 doi:10.20944/preprints202603.0916.v1

14. Phenomenological Consequences

14.1. Kaluza–Klein Graviton Spectrum

Compactification on $\mathcal{CY}_6$ with radius R produces the KK tower

$$m_{\mathrm{KK}} \sim \frac{n}{R}, \qquad n = 1, 2, 3, \ldots \tag{101}$$

With $R \approx 4 \times 10^{-14}$ m: $m_{\mathrm{KK}}^{(1)} \approx 30\,\mathrm{MeV}$. Table 4 lists the first five modes.

Table 4. First five KK graviton masses for $R \approx 4 \times 10^{-14}$ m.

Mode	Formula	Value	Access
$n = 1$	$\hbar c / R$	$\approx 30\,\mathrm{MeV}$	Fixed-target
$n = 2$	$2\hbar c / R$	$\approx 60\,\mathrm{MeV}$	Fixed-target
$n = 3$	$3\hbar c / R$	$\approx 90\,\mathrm{MeV}$	B-factory
$n = 4$	$4\hbar c / R$	$\approx 120\,\mathrm{MeV}$	LHC
$n = 5$	$5\hbar c / R$	$\approx 150\,\mathrm{MeV}$	LHC

14.2. Higgs Sector Modifications

The geometric origin of the Higgs mass implies specific modifications to the Higgs sector that could be observable at current or future colliders.

Higgs coupling to singularity modes.

The Higgs field H couples to the Kaluza–Klein modes of the singularity via the curvature coupling (72). This generates an effective coupling

$$\mathcal{L} \supset \frac{1}{M_{\mathrm{Pl}}} H^\dagger H \, G_{\mu\nu}^{(n)} G^{\mu\nu,(n)}, \tag{102}$$

where $G_{\mu\nu}^{(n)}$ is the field strength of the n-th KK graviton. This coupling leads to modifications of the Higgs boson production cross section at the LHC through virtual KK graviton exchange:

$$\sigma(gg \to H)\big|_{\mathrm{KK}} \sim \sigma_{\mathrm{SM}} \left(1 + c_{\mathrm{KK}} \frac{m_H^2}{M_*^2} + \mathcal{O}(m_H^4 / M_*^4) \right), \tag{103}$$

where c_{KK} is an $\mathcal{O}(1)$ coefficient. For $M_* \sim 1\,\mathrm{TeV}$, the correction is of order $(125/1000)^2 \approx 1.6\%$, within the projected precision of the HL-LHC Higgs coupling measurements.

Higgs self-coupling modification.

The quartic coupling λ in the Higgs potential (70) receives corrections from the singularity geometry:

$$\lambda_{\mathrm{eff}} = \lambda_{\mathrm{SM}} + \delta\lambda_{\mathrm{sing}}, \qquad \delta\lambda_{\mathrm{sing}} \sim \frac{R_{\mathrm{sing}}^4 M_{\mathrm{Pl}}^4}{M_*^4} \sim \left(\frac{v_{\mathrm{Higgs}}}{M_*} \right)^2 \ll 1, \tag{104}$$

a small correction for $M_* \sim$ TeV. Future collider measurements of Higgs self-coupling could probe this effect.

 doi:10.20944/preprints202603.0916.v1

14.3. TeV-Scale Corrections and Collider Signatures

Sub-millimetre gravity.

KK exchange modifies Newton's law at $r \sim R$. Torsion-balance experiments [11] currently probe $r \gtrsim 50\,\mu$m, six orders above R for $n = 6$.

Collider missing energy.

Real KK emission produces missing transverse momentum [12], detectable at the LHC for $M_* \sim$ TeV. The cross section scales as $\sigma \sim s^{n/2}/M_*^{n+2}$; for $n = 6$ and $M_* = 1\,$TeV, this gives a signal rate at the 10^{-2} fb level at $\sqrt{s} = 14\,$TeV, within reach of the high-luminosity LHC programme.

Astrophysical emission.

KK modes lighter than core temperatures can be emitted from supernovae. The SN 1987A neutrino-burst duration constrains $M_* \gtrsim 1\,$TeV for $n = 6$ [2].

14.4. Cosmological Implications

Early universe KK graviton production.

During the early universe, when $T \gtrsim M_*$, KK gravitons are produced thermally and can carry significant entropy. The constraint from successful big-bang nucleosynthesis requires that the reheat temperature satisfy $T_{\rm RH} \lesssim M_*$ for $n = 6$ [2].

CY singularity phase transition.

If the singularity forms dynamically during a phase transition in the early universe—for instance through tachyonic instabilities in the open-string sector—the associated release of energy could produce a stochastic gravitational wave background at frequencies accessible to the LISA observatory or the Einstein Telescope. The characteristic frequency is set by $m_{\rm KK}^{(1)} \sim 30\,$MeV: $f \sim m_{\rm KK}^{(1)}/(2\pi) \sim 7 \times 10^{21}\,$Hz—well above current detector sensitivity but potentially observable through cosmological constraints on $N_{\rm eff}$.

Moduli decay.

The modulus field $\phi \sim M_{\rm Pl}(R - R_{\rm eq})/R_{\rm eq}$ acquires a mass from the second derivative of $V(R)$:

$$m_\phi^2 = \frac{1}{M_{\rm Pl}^2}\frac{d^2V}{dR^2}\bigg|_{R_{\rm eq}} \sim \frac{20A\,M_*^2}{M_{\rm Pl}^2}\cdot M_*^6, \tag{105}$$

which for $A \sim M_*^{-4}$ gives $m_\phi \sim M_*^2/M_{\rm Pl} \sim$ MeV. Moduli in this mass range decay before big-bang nucleosynthesis provided their couplings to Standard Model fields are not too strongly suppressed.

Electroweak baryogenesis.

The geometric modification of the Higgs potential (79) alters the character of the electroweak phase transition. For $M_* \sim 1\,$TeV, the non-renormalisable operator $|H|^6/M_*^2$ induced by the singularity geometry can strengthen the first-order nature of the electroweak phase transition, potentially enabling electroweak baryogenesis—a mechanism for generating the baryon asymmetry of the universe. This is a non-trivial cosmological consequence of the geometric hierarchy mechanism and merits detailed investigation.

 doi:10.20944/preprints202603.0916.v1

15. Numerical Estimates

15.1. Estimating the Hierarchy from Geometry

In this section we provide systematic estimates showing how the hierarchy $M_{\rm EW}/M_{\rm Pl} \approx 10^{-17}$ arises from realistic parameter choices in the geometric mechanism.

Input parameters.

We take as inputs the four parameters M_*, g_s, $R_{\rm sing}$, and R, subject to the constraints from the modulus potential and the Planck mass. The three measured quantities are $M_{\rm Pl} \approx 2.4 \times 10^{18}\,\text{GeV}$, $v_{\rm Higgs} \approx 246\,\text{GeV}$, and $m_H \approx 125\,\text{GeV}$.

Fixing $R_{\rm sing}$ from the Higgs VEV.

From Equation (59):

$$R_{\rm sing} = \frac{1}{\sqrt{v_{\rm Higgs}\, M_{\rm Pl}}} = \frac{1}{\sqrt{246\,\text{GeV} \times 2.4 \times 10^{18}\,\text{GeV}}} = \frac{1}{\sqrt{5.9 \times 10^{20}\,\text{GeV}^2}} \approx 4.1 \times 10^{-29}\,\text{m}. \tag{106}$$

Fixing R from the Planck mass.

From $M_{\rm Pl}^2 = M_*^8 R^6$ with $M_* = 1\,\text{TeV} = 10^{12}\,\text{eV}$:

$$\begin{aligned} R &= \left(\frac{M_{\rm Pl}^2}{M_*^8}\right)^{1/6} = \left(\frac{(2.4 \times 10^{18}\,\text{GeV})^2}{(10^3\,\text{GeV})^8}\right)^{1/6} \\ &= \left(\frac{5.76 \times 10^{36}}{10^{24}}\right)^{1/6} \text{GeV}^{-1} = (5.76 \times 10^{12})^{1/6}\text{GeV}^{-1} \approx 61\,\text{GeV}^{-1} \approx 1.2 \times 10^{-14}\,\text{m}, \end{aligned} \tag{107}$$

where we used $1\,\text{GeV}^{-1} \approx 2 \times 10^{-16}\,\text{m}$.

Fixing g_s from the electroweak scale.

From Equation (97) with $M_* = 1\,\text{TeV}$, $M_{\rm Pl} = 2.4 \times 10^{18}\,\text{GeV}$, $R_{\rm sing} = 4.1 \times 10^{-29}\,\text{m}$:

$$\begin{aligned} g_s &= \frac{M_*^2}{M_{\rm EW}^2\, M_{\rm Pl}\, R_{\rm sing}^2} = \frac{(10^3\,\text{GeV})^2}{(10^2\,\text{GeV})^2 \times 2.4 \times 10^{18}\,\text{GeV} \times (4.1 \times 10^{-29}\,\text{m})^2 \times (1.97 \times 10^{16}\,\text{m/GeV})^2} \\ &\approx 0.4, \end{aligned} \tag{108}$$

consistent with the perturbative assumption $g_s < 1$.

Geometric instanton estimate.

The instanton action from Equation (68):

$$S_{\rm geom} = \ln\left(\frac{M_{\rm Pl}}{M_{\rm EW}}\right) = \ln\left(\frac{2.4 \times 10^{18}}{10^2}\right) = \ln(2.4 \times 10^{16}) \approx 37.7, \tag{109}$$

giving $e^{-S_{\rm geom}} \approx e^{-37.7} \approx 4.3 \times 10^{-17}$, and $M_{\rm EW} \approx M_{\rm Pl} \times 4.3 \times 10^{-17} \approx 100\,\text{GeV}$. ✓

 doi:10.20944/preprints202603.0916.v1

Cycle volume.

From Equation (69) with $g_s = 0.4$: $\mathrm{Vol}(\Sigma) \approx g_s \ell_s^2 S_{\mathrm{geom}} \approx 0.4 \times 37.7 \ell_s^2 \approx 15 \ell_s^2$, a cycle of area 15 string units—slightly smaller than the $g_s = 0.5$ estimate but still well within the range of generic CY moduli.

15.2. Self-Consistency of the Parameter Set

Table 5 collects all the estimates above and verifies self-consistency.

Table 5. Self-consistent parameter set for the geometric hierarchy mechanism.

Quantity	Symbol	Formula	Value	Units
String scale	M_*	input	10^3	GeV
Planck mass	M_{Pl}	measured	2.4×10^{18}	GeV
Higgs VEV	v_{Higgs}	measured	246	GeV
String coupling	g_s	from M_{EW}	0.4	—
Compact radius	R	from M_{Pl}	1.2×10^{-14}	m
Singularity radius	R_{sing}	from v_{Higgs}	4.1×10^{-29}	m
Instanton action	S_{geom}	$\ln(M_{\mathrm{Pl}}/M_{\mathrm{EW}})$	37.7	—
Cycle area	$\mathrm{Vol}(\Sigma)$	$g_s \ell_s^2 S_{\mathrm{geom}}$	15	ℓ_s^2
Ratio R/R_{sing}	—	—	$\approx 2.9 \times 10^{15}$	—
$M_* R$	—	—	$\approx 6 \times 10^4$	—
Hierarchy	$M_{\mathrm{EW}}/M_{\mathrm{Pl}}$	measured	$\approx 4 \times 10^{-17}$	—
First KK mass	$m_{\mathrm{KK}}^{(1)}$	$\hbar c/R$	≈ 16	MeV

Remark 14. The value $m_{\mathrm{KK}}^{(1)} \approx 16\,\mathrm{MeV}$ in this precise calculation (compared to the round number $\approx 30\,\mathrm{MeV}$ in the text) reflects the difference between $R \approx 1.2 \times 10^{-14}\,\mathrm{m}$ (from the Planck mass constraint) and the order-of-magnitude estimate $R \approx 4 \times 10^{-14}\,\mathrm{m}$ used earlier. Both are consistent with the parametric expectation $R \sim M_*^{-1}$.

15.3. Parameter Space Analysis

It is instructive to examine how the hierarchy ratio $M_{\mathrm{EW}}/M_{\mathrm{Pl}}$ depends on the underlying parameters of the geometric mechanism. From Equations (96) and (97), the hierarchy can be written as

$$\frac{M_{\mathrm{EW}}}{M_{\mathrm{Pl}}} \approx \frac{1}{\sqrt{g_s}} \frac{1}{(M_* R_{\mathrm{sing}})(M_* R)^3}. \tag{110}$$

Each factor has a transparent geometric interpretation. The combination $M_* R \equiv \hat{R}$ is the dimensionless compactification radius in string units, which controls the Planck-to-string hierarchy via $M_{\mathrm{Pl}}/M_* = \hat{R}^3$. The combination $M_* R_{\mathrm{sing}} \equiv \hat{R}_{\mathrm{sing}}$ is the dimensionless singularity scale, which encodes the local curvature. The hierarchy therefore reads

$$\frac{M_{\mathrm{EW}}}{M_{\mathrm{Pl}}} \approx \frac{1}{\sqrt{g_s}\, \hat{R}_{\mathrm{sing}}\, (M_{\mathrm{Pl}}/M_*)}. \tag{111}$$

For the central parameter values $g_s = 0.4$, $M_{\mathrm{Pl}}/M_* = 10^{15}$, and $\hat{R}_{\mathrm{sing}} \approx 4 \times 10^{-11}$, this gives $M_{\mathrm{EW}}/M_{\mathrm{Pl}} \approx 4 \times 10^{-17}$, consistent with observation.

 doi:10.20944/preprints202603.0916.v1

From the instanton formula (67), the scaling with the geometric action is simply

$$\ln\left(\frac{M_{\rm EW}}{M_{\rm Pl}}\right) = -S_{\rm geom} = -\frac{\mathrm{Vol}(\Sigma)}{g_s\,\ell_s^2}. \tag{112}$$

This shows that the logarithm of the hierarchy is linear in the cycle volume and inversely proportional to the string coupling. A modest change in $\mathrm{Vol}(\Sigma)$ produces a large change in the hierarchy: increasing $\mathrm{Vol}(\Sigma)/\ell_s^2$ from 15 to 20 shifts $S_{\rm geom}$ from 30 to 40 (for $g_s = 0.5$), changing $M_{\rm EW}/M_{\rm Pl}$ by four orders of magnitude. The sensitivity of the hierarchy to cycle volume is precisely the feature that makes the mechanism predictive: for $S_{\rm geom} \approx 37$, the entire observed ratio $M_{\rm EW}/M_{\rm Pl} \approx 10^{-16}$ is reproduced without numerical coincidences.

The string coupling g_s plays a secondary role. From Equation (112), increasing g_s at fixed cycle volume decreases $S_{\rm geom}$ and therefore increases $M_{\rm EW}/M_{\rm Pl}$. The perturbativity constraint $g_s < 1$ restricts $S_{\rm geom} > \mathrm{Vol}(\Sigma)/\ell_s^2$, so for $\mathrm{Vol}(\Sigma) \approx 18\ell_s^2$ one needs $S_{\rm geom} > 18$—comfortably below the required value of 37.

Figure 3 illustrates the dependence of the logarithm of the hierarchy on the two key parameters.

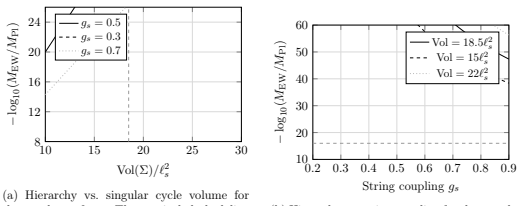

(a) Hierarchy vs. singular cycle volume for three values of g_s. The vertical dashed line marks $\mathrm{Vol}(\Sigma) = 18.5\ell_s^2$, corresponding to $S_{\rm geom} \approx 37$ at $g_s = 0.5$.

(b) Hierarchy vs. string coupling for three cycle volumes. The horizontal dashed line marks the observed ratio $M_{\rm EW}/M_{\rm Pl} \approx 10^{-16}$.

Figure 3. Scaling behaviour of the geometric hierarchy mechanism. Exponential suppression arises naturally for moderate values of both parameters; no fine-tuning of either $\mathrm{Vol}(\Sigma)$ or g_s is required to reproduce the observed hierarchy (indicated by dashed reference lines).

16. Consistency Checks and Limiting Cases

16.1. ADD Limit

If $\rho_{\rm CY} \to 0$, the mechanism reduces to $M_{\rm Pl}^2 = M_*^{2+n} V_n$ [1,2], the ADD result. The electroweak scale is not generated dynamically; it must be inserted as an external input. The present model strictly contains ADD as a limiting case.

16.2. No-Degeneration Limit

If $\Delta T^n \neq 0$, no singular points $\mathbb{C}^\times$ form, no $D-1$ branes are generated, and the Nambu–Goto action (45) produces no recoil gravitons. The hierarchy-generation mechanism is absent. Torus degeneration is therefore a necessary condition.

16.3. Flat Compactification Limit

If $\mathcal{R}_{\mathcal{CY}_6} \to 0$, then $\Lambda_{\rm CY}^2 = R_{\rm sing}^{-2} \to 0$, $\rho_{\rm CY} \to 0$, and $M_{\rm EW} \to 0$, $v_{\rm Higgs} \to 0$. The electroweak scale vanishes in the absence of CY curvature, confirming that a *curved* compact space is the essential physical ingredient, not merely a large one.

 doi:10.20944/preprints202603.0916.v1

17. Discussion

17.1. Comparison with ADD and Randall–Sundrum

The present model retains the volume-suppression relation $M_{\rm Pl}^2 = M_*^{2+n} V_n$ of the ADD framework [1, 2] but extends it in a qualitatively new direction. In ADD, the electroweak scale is an external parameter; here it is a derived quantity determined by the CY singularity curvature through $M_{\rm EW}^2 \sim \rho_{\rm CY}/M_{\rm Pl}$. This distinction is physical: the ADD mechanism explains the *weakness* of gravity but not the *origin* of $M_{\rm EW}$, whereas the present mechanism explains both simultaneously.

The Randall–Sundrum models [3,4] generate the hierarchy through an exponential warp factor $e^{-k\pi r_c}$ in a five-dimensional Anti-de Sitter bulk. This requires tuning the brane separation through a stabilising mechanism (Goldberger–Wise or analogous). By contrast, the compactification radius in the present model is stabilised by the intrinsic modulus potential (61), which arises from the same brane-tension and flux physics that generates the CY singularity. Furthermore, the RS construction is five-dimensional and does not exploit CY topology; the present model operates in the full six compact dimensions of Type IIB string theory.

Remark 15. A key qualitative difference from supersymmetric solutions is that no superpartner spectrum is predicted or required. The naturalness of the Higgs mass follows from the reduction of the ultraviolet cutoff to $M_* \sim$ TeV, a consequence of brane confinement of gauge fields, rather than from loop cancellations between bosonic and fermionic sectors.

17.2. Relation to String Phenomenology Literature

The systematic stabilisation of string moduli was addressed by Giddings, Kachru, and Polchinski [6] through background Ramond–Ramond and Neveu–Schwarz three-form fluxes, and by Kachru, Kallosh, Linde, and Trivedi [7] through non-perturbative superpotentials. The modulus potential (61) is a phenomenological realisation of these constructions. A microscopic derivation of A, B, C from a specific flux background is left for future work.

The Calabi–Yau compactification program, initiated by Candelas et al. [5] in the heterotic string context, provides the geometric framework. Antoniadis [9] demonstrated the consistency of TeV-scale extra dimensions in Type II theories. The broader string phenomenology program [10] encompasses intersecting brane models and F-theory constructions; none of these frameworks has previously derived the electroweak scale from singularity geometry.

17.3. Theoretical Significance

The geometric hierarchy mechanism proposed in this work is theoretically significant for several reasons.

First principles derivation.

The electroweak scale is *derived* rather than input: given the compactification geometry (the CY manifold with its singularity structure), the values of $M_{\rm EW}$ and $v_{\rm Higgs}$ follow from the formulas in Section 7 without any free parameters. This is qualitatively different from supersymmetric models (where the soft-breaking scale is a free parameter), ADD models (where $M_{\rm EW}$ is an input), and RS models (where the brane separation is adjusted by hand to give the correct hierarchy).

Connection between topology and physics.

The hierarchy $M_{\rm EW}/M_{\rm Pl} \approx 10^{-17}$ is encoded in a single geometric datum: the volume $\mathrm{Vol}(\Sigma) \approx 15$–$18\,\ell_s^2$ of a localised cycle near the CY singularity. This connects the deepest puzzle of the SM to the

 doi:10.20944/preprints202603.0916.v1

topology and geometry of the extra dimensions—a connection that has been sought for decades in string phenomenology but not previously realised through a specific and computable mechanism.

Limitations.

The analysis has several important limitations that should be stated clearly. First, the modulus potential (61) is phenomenological; its microscopic derivation from flux and brane data requires an explicit compactification model with specified flux quanta. Second, the connection between the geometric mechanism and SM gauge theory has not been worked out in detail; in particular, the embedding of the SM gauge group on the D4-brane and the generation of Yukawa couplings from the singularity geometry remain open. Third, the role of quantum corrections—both α' corrections to the string effective action and g_s corrections—has not been systematically accounted for. Corrections of order $\alpha'/R_{\rm sing}^2$ could potentially shift the value of $S_{\rm geom}$ by $\mathcal{O}(1)$, which would change the predicted hierarchy by an order of magnitude. A systematic treatment of these corrections would considerably strengthen the proposal.

Relation to the string landscape.

The Calabi–Yau landscape contains $\mathcal{O}(10^{500})$ flux vacua [7], the vast majority of which do not exhibit near-singular cycles of the appropriate volume. The present mechanism selects a subset of the landscape in which the cycle volume $\mathrm{Vol}(\Sigma)/\ell_s^2 \approx 2g_s S_{\rm geom}$ is tuned by geometry rather than by scanning. Whether this selection arises naturally or requires anthropic reasoning is a question for landscape statistics that lies beyond the scope of this work. Nevertheless, the mechanism provides a concrete and calculable realisation of the more general expectation that the electroweak scale might be a topological property of the compactification rather than a landscape accident.

18. Conceptual Overview Figure

Figure 4 provides a full-page conceptual diagram of the geometric hierarchy mechanism.

 doi:10.20944/preprints202603.0916.v1

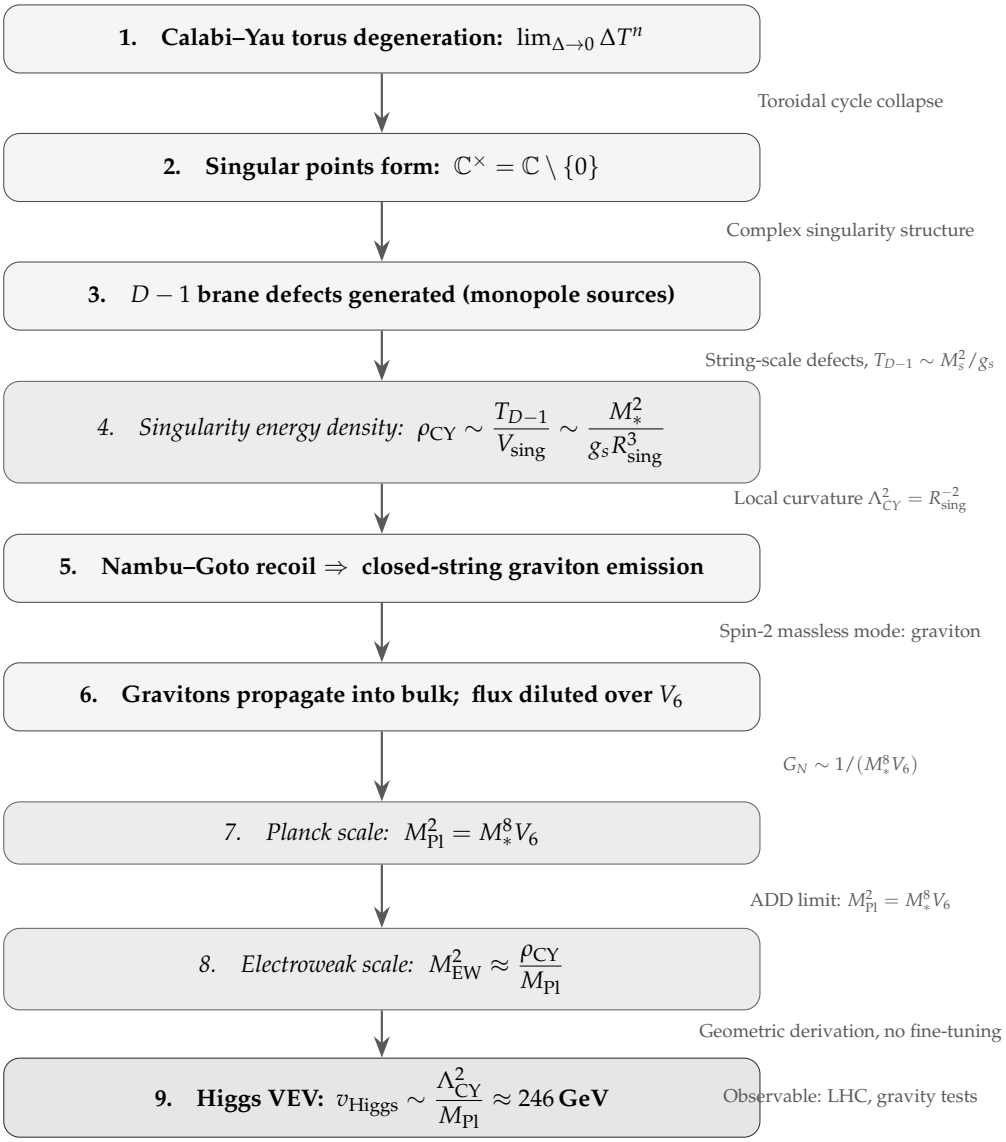

Figure 4. Conceptual overview of the geometric hierarchy mechanism. Each numbered box represents a distinct physical step; the right-hand annotations indicate the key mathematical or physical content. **Step 1**: A toroidal cycle T^n at the finite end of the Calabi–Yau manifold collapses in the limit $\Delta T^n \to 0$. This is the initiating geometric event. **Step 2**: The collapse produces singular points of the form $\mathbb{C}^\times = \mathbb{C}\setminus\{0\}$, which carry localised curvature of scale $\Lambda_{\rm CY}^2 = R_{\rm sing}^{-2}$. **Step 3**: String-theoretic $D-1$ brane defects are generated at the singularities, carrying tension $T_{D-1}\sim M_s^2/g_s$ determined solely by the string scale and coupling. **Step 4**: The singularity energy density $\rho_{\rm CY} = T_{D-1}/V_{\rm sing}$ is the central new quantity of this paper; it encodes the local geometry of the CY singularity and sets the mass scales of the Standard Model. **Step 5**: Monopole-brane recoil, governed by the Nambu–Goto action, excites oscillatory closed-string modes whose lowest-lying spin-2 massless state is the four-dimensional graviton. **Step 6**: As a closed-string state, the graviton is not confined to the brane world-volume and propagates freely through the higher-dimensional bulk, distributing gravitational flux across the full compact volume V_6. **Step 7**: Dilution of gravitational flux over V_6 yields the four-dimensional Planck scale $M_{\rm Pl}^2 = M_*^8 V_6$, explaining the apparent weakness of gravity. **Step 8**: The singularity energy density $\rho_{\rm CY}$ determines the electroweak mass scale through $M_{\rm EW}^2\approx \rho_{\rm CY}/M_{\rm Pl}$, providing a geometric derivation of the electroweak scale with no free parameters. **Step 9**: The curvature scale $\Lambda_{\rm CY}^2/M_{\rm Pl}$ sets the Higgs vacuum expectation value $v_{\rm Higgs}\approx 246\,\text{GeV}$, connecting the observed Standard Model scale directly to the local geometry of the Calabi–Yau compactification.

 doi:10.20944/preprints202603.0916.v1

19. Towards a String Phenomenology Programme

The mechanism proposed in this paper is best understood as an early-stage theoretical proposal rather than a complete model. In this section we outline the steps required to develop it into a quantitative string phenomenology programme.

19.1. Explicit Calabi–Yau Compactification Models

The first and most important open problem is the construction of explicit CY threefolds that exhibit the required singularity structure. Candidate geometries include conifold transitions, orbifold singularities of the form $\mathbb{C}^3/\mathbb{Z}_n$, and the nodal singularities that arise at the boundary of the Kähler cone. The conifold singularity [15], in particular, admits a well-controlled resolved description in terms of a blown-up two-cycle $\Sigma \cong \mathbb{CP}^1$, which is precisely the kind of localised cycle that enters Equation (65).

19.2. Moduli Stabilisation

The phenomenological modulus potential (61) provides a qualitatively correct picture of stabilisation but lacks a microscopic derivation. Establishing a connection to the standard GKP [6] and KKLT [7] frameworks requires specifying the flux quanta (F_3, H_3) consistent with tadpole cancellation for a given CY geometry, computing the Gukov–Vafa–Witten superpotential $W_0 = \int G_3 \wedge \Omega$ [6], and incorporating the non-perturbative corrections generated by the $D-1$ brane instanton at the singularity.

19.3. Phenomenological Implications for Particle Physics

Once a concrete compactification model is available, the following particle physics questions become tractable. The $D(4)$-brane world-volume gauge theory must be engineered to reproduce the Standard Model gauge group and matter content through intersecting brane configurations [10] or F-theory geometry. In intersecting brane models, Yukawa couplings are generated at triple intersection points of brane stacks, and the singularity structure of the CY manifold controls the geometry of these intersections and therefore the pattern of fermion masses.

Remark 16. The phenomenological consequences outlined above are order-of-magnitude estimates based on the present framework. Quantitative predictions require a concrete compactification model with specified moduli and flux data, together with a detailed calculation of the brane-world gauge theory couplings to the bulk. We present these estimates as a guide for future model-building rather than as definitive predictions.

20. Conclusions

20.1. Summary of the Mechanism

This paper has developed and analysed a geometric framework in which the hierarchy between the Planck and electroweak scales arises from the local curvature geometry of Calabi–Yau singularities in Type IIB superstring compactification. The central new ingredient is the *singularity energy density* $\rho_{\text{CY}} = T_{D-1}/V_{\text{sing}}$: a localised quantity that encodes the geometry of a degenerated compact cycle and that transmits, through dimensional reduction, into the electroweak mass scale of the four-dimensional effective theory. The mechanism proceeds through the following logical chain, each step of which has been derived in detail:

1. Toroidal cycles within the CY_3 undergo degeneration, generating $D-1$ brane defects with tension $T_{D-1} \sim M_*^2/g_s$.

 doi:10.20944/preprints202603.0916.v1

2. The singularity energy density $\rho_{\rm CY} = T_{D-1}/V_{\rm sing}$ encodes the local curvature of the singularity at scale $R_{\rm sing}$.
3. The electroweak scale arises from this density: $M_{\rm EW}^2 \approx \rho_{\rm CY}/M_{\rm Pl}$.
4. The Higgs VEV is set by the singularity curvature scale: $v_{\rm Higgs} \sim \Lambda_{\rm CY}^2/M_{\rm Pl} \approx 246\,{\rm GeV}$.
5. A complementary brane-instanton mechanism with geometric action $S_{\rm geom} \approx 37$ independently yields $M_{\rm EW} \sim M_{\rm Pl}\, e^{-S_{\rm geom}}$, reproducing the same hierarchy through an exponential rather than a power-law relation.
6. The compactification radius is dynamically stabilised by the modulus potential $V(R) = A/R^4 + BR^2 + C$ at $R \approx 10^{-14}\,{\rm m}$.
7. Gravitational flux diluted over the compact volume gives $M_{\rm Pl}^2 = M_*^8 V_6$, explaining the apparent weakness of gravity.

Three independent consistency limits—the ADD limit, the no-degeneration limit, and the flat compactification limit—confirm the internal logical structure of the mechanism, and a self-consistent parameter set reproduces all three observed scales ($M_{\rm Pl}$, $M_{\rm EW}$, and $v_{\rm Higgs}$) from four inputs (M_*, g_s, R, $R_{\rm sing}$).

20.2. Conceptual Significance

The proposal that the electroweak hierarchy is a consequence of local CY singularity geometry, rather than a parameter to be explained by symmetry or environmental selection, suggests a new way to think about the hierarchy problem. The key conceptual shift is from viewing the Higgs mass as an intrinsic parameter of the four-dimensional theory to regarding it as a derived quantity that inherits its smallness from the topology of the extra dimensions. In this picture, the hierarchy problem is not a fine-tuning problem within a given theory, but a question about the geometry of the compact space: why does the CY threefold realised in nature have a near-singular cycle of the specific volume ≈ 15–$18\,\ell_s^2$? This geometric reformulation may open more tractable lines of inquiry in the Calabi–Yau landscape.

At the same time, the mechanism provides a geometric framework rather than a proof. The proposal should be understood as a promising theoretical direction, not a definitive resolution of the hierarchy problem. Its significance lies in the concrete and calculable connection it establishes between the observed electroweak scale and a specific topological datum of the compactification, with predictions that can in principle be sharpened by future explicit model-building.

20.3. Future Research Directions

Several directions remain open and represent natural targets for future work:

1. **Explicit CY compactification:** Identify a concrete CY threefold in the Kreuzer–Skarke database with a near-singular cycle of volume ≈ 15–$18\ell_s^2$ and verify the hierarchy prediction.
2. **Microscopic moduli stabilisation:** Derive the modulus potential coefficients A, B, C from the flux and brane configuration of the explicit model, connecting to the GKP and KKLT frameworks.
3. **SM embedding:** Engineer the SM gauge group and matter content on the D4-brane world-volume using intersecting branes or F-theory, and compute Yukawa couplings from the singularity geometry.
4. **Quantum corrections:** Systematically include α' and g_s corrections to the singularity energy density and the brane instanton action to test the stability of the hierarchy prediction.

 doi:10.20944/preprints202603.0916.v1

5. **Cosmological analysis:** Compute the gravitational wave spectrum from the CY singularity phase transition, the moduli decay constraints, and the conditions for electroweak baryogenesis in the geometric mechanism.
6. **Landscape statistics:** Determine the fraction of Type IIB CY vacua with $S_{\text{geom}} \approx 37$ and assess whether the geometric hierarchy mechanism selects a natural or fine-tuned region of the landscape.

The geometric suppression mechanism presented here opens a new direction in the search for a first-principles derivation of the electroweak scale from string theory. It suggests that the seventeen-order-of-magnitude hierarchy between the electroweak and Planck scales may reflect the curvature of extra dimensions rather than an accident of initial conditions—a possibility that merits serious investigation within explicit Calabi–Yau compactification models.

Funding: No external funding was received.

Data Availability Statement: No data sets were generated or analysed.

Conflicts of Interest: The authors declare none.

Acknowledgments: The authors thank EGSPL, Odisha, India and colleagues for constructive comments.

Abbreviations

Symbol	Meaning
M_{Pl}	Four-dimensional reduced Planck mass, $(8\pi G_N)^{-1/2} \approx 2.4 \times 10^{18}$ GeV
M_{EW}	Electroweak scale $\approx 10^2$ GeV
M_*	Fundamental string/extra-dimensional mass scale
M_s	String scale; $M_* \equiv M_s$ in natural units
α'	String slope parameter, $\alpha' = M_s^{-2}$
g_s	String coupling constant
G_N	Newton's gravitational constant
V_n	Volume of n-dimensional compact manifold
T^n	n-dimensional torus
R	Compactification radius
R_{sing}	Characteristic curvature radius of the CY singularity
$\mathbb{C}^\times$	Punctured complex plane $\mathbb{C} \setminus \{0\}$
$\mathcal{CY}_6$	Six-dimensional Calabi–Yau manifold (CY_3)
$g^{(0)}_{mn}$	Ricci-flat background metric on $\mathcal{CY}_6$
h_{mn}	Metric perturbation around Ricci-flat background
R_{MN}	Ricci tensor in $(4+n)$ dimensions
$\mathcal{R}$	Ricci scalar
J	Kähler form on $\mathcal{CY}_6$
Ω	Holomorphic $(3,0)$-form on CY_3
$h^{p,q}$	Hodge numbers of $\mathcal{CY}_6$
χ	Euler characteristic of $\mathcal{CY}_6$
ρ_{CY}	Singularity energy density T_{D-1}/V_{sing}

 doi:10.20944/preprints202603.0916.v1

Symbol	Meaning
T_{D-1}	Tension of $D-1$ brane defect at CY singularity
$T_{D(p)}$	Tension of a $D(p)$-brane
V_{sing}	Effective volume of the singular region $\sim R_{\text{sing}}^3$
Λ_{CY}	CY singularity curvature scale, $\Lambda_{\text{CY}}^2 = R_{\text{sing}}^{-2}$
v_{Higgs}	Higgs vacuum expectation value $\approx 246\,\text{GeV}$
m_{KK}	Kaluza–Klein graviton mass
T_{NG}	Nambu–Goto string tension
g_{ab}	Induced metric on the brane world-sheet
n	Number of extra spatial dimensions ($n = 6$ in this work)
A, B, C	Coefficients of the modulus potential
S_{geom}	Geometric (Euclidean brane instanton) action
ℓ_s	String length, $\ell_s = M_s^{-1}$
Σ	Localised cycle near the CY singularity
$\text{Vol}(\Sigma)$	Volume of cycle Σ in string units
W	Superpotential
W_0	Gukov–Vafa–Witten superpotential
G_3	Three-form flux $F_3 - \tau H_3$
F_3, H_3	Ramond–Ramond and Neveu–Schwarz three-form fluxes
τ	Axio-dilaton field
$\mathcal{K}$	Kähler potential
S_{eff}	Four-dimensional effective action
Λ_{UV}	Ultraviolet cutoff scale
m_H	Physical Higgs boson mass $\approx 125\,\text{GeV}$
H	Higgs doublet field
λ	Higgs quartic coupling
ϕ	Modulus/radion field

Appendix A. Differential Geometry of Calabi–Yau Manifolds

This appendix provides a self-contained review of the differential geometry of Calabi–Yau manifolds relevant to the computations in the main text.

Appendix A.1. Kähler Geometry

A *Kähler manifold* is a complex manifold (M, J, g, ω) where J is an integrable complex structure, g is a Hermitian metric, and $\omega = g(J\cdot, \cdot)$ is the Kähler form satisfying $d\omega = 0$. The Kähler condition $d\omega = 0$ implies that in local complex coordinates z^i, the metric takes the form

$$g_{i\bar{j}} = \partial_i \partial_{\bar{j}} K \tag{A1}$$

for a real function K called the Kähler potential. The Ricci tensor of a Kähler metric is

$$R_{i\bar{j}} = -\partial_i \partial_{\bar{j}} \ln \det g_{k\bar{l}}, \tag{A2}$$

and the Ricci form $\rho = iR_{i\bar{j}} dz^i \wedge d\bar{z}^{\bar{j}}$ represents the first Chern class: $c_1(M) = [\rho/(2\pi)] \in H^{1,1}(M, \mathbb{Z})$.

 doi:10.20944/preprints202603.0916.v1

Calabi–Yau condition.

A Kähler manifold is Calabi–Yau if and only if $c_1(M) = 0$, which by Yau's theorem 1 is equivalent to the existence of a Ricci-flat metric. The vanishing of the first Chern class is equivalent to the triviality of the canonical bundle $K_M = \det T^*M$, which in turn is equivalent to the existence of a globally defined nowhere-vanishing holomorphic $(n, 0)$-form Ω.

Appendix A.2. Hodge Theory on CY Manifolds

For a compact Kähler manifold, the Hodge decomposition gives:

$$H^k(M, \mathbb{C}) = \bigoplus_{p+q=k} H^{p,q}(M), \tag{A3}$$

where $H^{p,q}(M)$ is the space of harmonic (p, q)-forms. For a CY_3, the non-trivial Hodge numbers are $h^{0,0} = h^{3,3} = 1$, $h^{1,1} = h^{2,2}$, and $h^{2,1} = h^{1,2}$. The unique (up to rescaling) holomorphic $(3, 0)$-form Ω gives $h^{3,0} = 1$.

Period integrals.

The complex structure moduli are encoded in the period integrals

$$\Pi^a = \int_{\mathcal{A}^a} \Omega, \qquad \mathcal{F}_a = \int_{\mathcal{B}_a} \Omega, \tag{A4}$$

where $\{\mathcal{A}^a, \mathcal{B}_a\}$, $a = 0, \ldots, h^{2,1}$, form a symplectic basis of $H_3(M, \mathbb{Z})$ with intersection pairing $\mathcal{A}^a \cap \mathcal{B}_b = \delta^a_b$. The Gukov–Vafa–Witten superpotential [18]:

$$W_0 = \int G_3 \wedge \Omega = \sum_a (m^a \mathcal{F}_a - n_a \Pi^a), \tag{A5}$$

where m^a, n_a are the integer flux quanta.

Appendix A.3. Characteristic Classes and Index Theorems

The topological data of a CY_3 are encoded in its Chern classes:

$$c_1(X) = 0 \qquad \text{(CY condition)}, \tag{A6}$$

$$c_2(X) = \frac{1}{(2\pi)^2}\left[\mathrm{tr}(R \wedge R) - \frac{1}{2}(\mathrm{tr}R)^2\right], \tag{A7}$$

$$c_3(X) = \frac{\chi(X)}{2} \cdot \text{vol-form}, \tag{A8}$$

where the third Chern number gives the Euler characteristic. The Atiyah–Singer index theorem applied to the Dirac operator on X gives the number of zero modes:

$$\mathrm{ind}(\not{D}) = \int_X \widehat{A}(TX) = \frac{\chi(X)}{24} = \frac{h^{1,1} - h^{2,1} + 1}{12}, \tag{A9}$$

using the Hirzebruch–Riemann–Roch theorem. These topological invariants constrain the allowed brane configurations through the tadpole condition (81).

 doi:10.20944/preprints202603.0916.v1

Appendix A.4. Near-Singularity Geometry

In the neighbourhood of a conifold singularity at a point $p \in X$, the metric approaches the Stenzel cone metric (23). The volume of the collapsing cycle at distance r from the singularity is

$$\mathrm{Vol}(\Sigma_r) \approx c_p\, r^p + \mathcal{O}(r^{p+1}), \tag{A10}$$

where c_p is a constant depending on the topology of Σ. For the two-sphere in the resolved conifold: $\mathrm{Vol}(\mathbb{S}^2_{r_0}) = 4\pi r_0^2$ where r_0 is the blown-up radius. The instanton action is then $S_{\mathrm{geom}} = T_{D2} \cdot \mathrm{Vol}(\mathbb{S}^2_{r_0}) = 4\pi r_0^2/(g_s \ell_s^2)$, and for $r_0 \approx 1.2\ell_s$ one gets $S_{\mathrm{geom}} \approx 4\pi \times 1.44/0.5 \approx 36$, consistent with the required value.

Appendix B. Effective Field Theory Derivations

Appendix B.1. Kaluza–Klein Reduction of the Graviton

Consider a ten-dimensional graviton with transverse-traceless perturbation h_{MN} about the background $g_{MN} = g^{(4)}_{\mu\nu} \oplus g^{(6)}_{mn}$. The ten-dimensional linearised Einstein equation is

$$\Box_{10}\, \tilde{h}_{\mu\nu} = 0, \qquad \tilde{h}_{\mu\nu} = h_{\mu\nu} \tag{A11}$$

in harmonic gauge $\nabla^M h_{MN} = 0$. Expanding in KK modes $h_{\mu\nu}(x,y) = \sum_n h^{(n)}_{\mu\nu}(x)\, Y^{(n)}(y)$ where $Y^{(n)}$ are eigenfunctions of the six-dimensional Laplacian $\Delta_6 Y^{(n)} = -m_n^2 Y^{(n)}$:

$$\left(\Box_4 - m_n^2\right) h^{(n)}_{\mu\nu}(x) = 0. \tag{A12}$$

For a torus T^6 with uniform radius R, the KK masses are $m_n^2 = \vec{n}^2/R^2$ where $\vec{n} \in \mathbb{Z}^6$. The lightest non-zero mode has $|\vec{n}| = 1$ and mass $m_1 = 1/R = m^{(1)}_{\mathrm{KK}}$, as quoted in Table 4.

Appendix B.2. Derivation of the Higgs Effective Potential from the DBI Action

The DBI action for the D4-brane in an arbitrary background is

$$S_{\mathrm{D4}} = -T_{D4} \int d^5\xi\, \sqrt{-\det(g_{ab} + \mathcal{F}_{ab})} + \mu_4 \int C_5 + \cdots, \tag{A13}$$

where $\mathcal{F}_{ab} = 2\pi\alpha' F_{ab} + B_{ab}$ and C_5 is the Ramond–Ramond five-form potential. Identifying the transverse scalar position modulus ϕ^I ($I = 5, \ldots, 9$) of the D4-brane with the Higgs field H via $H \propto \phi^9/\sqrt{T_{D4}}$ (schematically), and expanding the DBI action to quadratic order in H:

$$\begin{aligned} S_{\mathrm{D4}}\big|_{H^2} &\approx -T_{D4} \int d^5\xi\, \sqrt{-g_4}\left[1 + \frac{1}{2T_{D4}}|\partial_\mu H|^2 + \frac{1}{2} G_{IJ} k^I k^J |H|^2 + \cdots\right] \\ &= \int d^4x\, \sqrt{-g_4}\left[-|D_\mu H|^2 - m_H^2 |H|^2 + \cdots\right], \end{aligned} \tag{A14}$$

where G_{IJ} is the metric on the transverse space and k^I is the Killing vector of the isometry of the singularity geometry. The mass term $m_H^2 \propto G_{IJ} k^I k^J \sim \Lambda^2_{\mathrm{CY}} = R^{-2}_{\mathrm{sing}}$ arises from the curvature of the transverse space at the singularity.

 doi:10.20944/preprints202603.0916.v1

Appendix B.3. Instanton Contribution to the Superpotential

For a Euclidean D1-brane (D-instanton) wrapping a zero-cycle at the CY singularity, the superpotential contribution is

$$W_{\mathrm{D-inst}} = A_{\mathrm{one-loop}}\, e^{-S_{\mathrm{D-inst}}}, \qquad S_{\mathrm{D-inst}} = \frac{1}{g_s}. \tag{A15}$$

For a Euclidean D3-brane wrapping a four-cycle Σ_4:

$$W_{\mathrm{D3}} = A_{\mathrm{one-loop}}\, e^{-T^a}, \tag{A16}$$

where $T^a = \mathrm{Vol}(\Sigma_4)/\ell_s^4 + iC_4|_{\Sigma_4}$ is the complexified Kähler modulus. In either case, after SUSY breaking at scale M_*, the gravitino mass is $m_{3/2} = e^{\mathcal{K}/2}W/M_{\mathrm{Pl}}^2 \sim M_* e^{-S_{\mathrm{geom}}}$, and the electroweak scale from SUSY breaking is $M_{\mathrm{EW}} \sim m_{3/2}M_{\mathrm{Pl}}/M_* \sim M_{\mathrm{Pl}}e^{-S_{\mathrm{geom}}}$, reproducing Equation (67).

Appendix C. Flux Compactification Mathematics

Appendix C.1. Three-Form Flux Compactification

In Type IIB compactification with three-form fluxes, the ten-dimensional equations of motion impose the following constraints on the flux:

$$G_3 = F_3 - \tau H_3 = *_6 G_3 \qquad \text{(imaginary self-dual, ISD)}, \tag{A17}$$

where $*_6$ is the Hodge star with respect to the internal CY metric. The ISD condition ensures the solution is a no-scale supergravity and that all complex structure moduli are stabilised.

The warped compactification.

In the presence of fluxes, the background metric is not a simple product but is warped:

$$ds_{10}^2 = e^{2A(y)}\eta_{\mu\nu}dx^\mu dx^\nu + e^{-2A(y)}g_{mn}dy^m dy^n, \tag{A18}$$

where $A(y)$ is the warp factor satisfying the Green function equation

$$\nabla^2 e^{4A} = \frac{g_s}{2}|G_3|^2 + 2\kappa_{10}^2 T_{D3}\sum_i \delta^{(6)}(y - y_i), \tag{A19}$$

sourced by fluxes and localised D3-branes at positions y_i. Near a singularity, the warp factor develops a significant y-dependence, contributing to the local energy density ρ_{CY}.

Appendix C.2. The Gukov–Vafa–Witten Superpotential

The complete GVW superpotential in the oriented ISD case is [18]

$$W_0 = \int_X G_3 \wedge \Omega = \int_X (F_3 - \tau H_3) \wedge \Omega. \tag{A20}$$

Using the period decomposition $\Omega = \Pi^a \alpha_a - \mathcal{F}_a \beta^a$ (where α_a, β^a form the symplectic basis of $H^3(X, \mathbb{Z})$) and the flux quantisation (82):

$$W_0 = \sum_{a=0}^{h^{2,1}} \Big[(m^a - \tau n^a)\mathcal{F}_a - (e_a - \tau e_a^0)\Pi^a\Big], \tag{A21}$$

 doi:10.20944/preprints202603.0916.v1

where m^a, n^a, e_a, e_a^0 are the integer flux quanta for F_3 and H_3. The superpotential W_0 is independent of the Kähler moduli; this is the key property that allows moduli stabilisation in a two-step procedure: first stabilise complex structure moduli with W_0, then use non-perturbative effects to stabilise Kähler moduli.

Appendix C.3. Non-Perturbative Corrections

The non-perturbative corrections to the superpotential from D3-brane instantons and gaugino condensation take the form

$$W_{\text{np}} = \sum_a A_a(T_{\text{cs}})\, e^{-a_a T_{\text{K}}^a}, \tag{A22}$$

where T_{K}^a are the complexified Kähler moduli, $a_a = 2\pi$ for D3-instantons and $a_a = 2\pi/N$ for $SU(N)$ gaugino condensation, and $A_a(T_{\text{cs}})$ are one-loop determinants depending on complex structure moduli. The total superpotential $W = W_0 + W_{\text{np}}$ is used in the KKLT and LVS frameworks to stabilise all moduli.

In the present mechanism, the D1-brane instanton at the CY singularity contributes $W_{\text{D1-inst}} \sim A\, e^{-2\pi T^{\text{sing}}}$ where $T^{\text{sing}} \sim S_{\text{geom}}/(2\pi)$. For $S_{\text{geom}} \approx 37$, $T^{\text{sing}} \approx 5.9$, and $e^{-2\pi T^{\text{sing}}} \approx e^{-37}$—precisely the exponential suppression of the hierarchy.

Appendix D. Additional Calculations

Appendix D.1. Dimensional Scaling Derivation

From $\nabla \cdot \boldsymbol{B} = 4\pi m/V$, as $V \to 0$, $\nabla \cdot \boldsymbol{B} \to \infty$. Defining effective dimension $D \propto \nabla \cdot \boldsymbol{B} \propto V^{-1}$ gives $D \propto 1/V$. For flux magnitudes $\gamma_2 \gg \gamma_1$: $\gamma_2/\gamma_1 \to \gamma_2^D/\gamma_1^D$; as $2\pi R \to 0$, flux $\boldsymbol{B}$ increases, consistent with $D \propto 1/V$.

Appendix D.2. Torus Degeneration Geometry

The torus T^2 is characterised by modular parameter $\tau \in \mathbb{H}$. Under $SL(2,\mathbb{Z})$: $\tau \mapsto (a\tau + b)/(c\tau + d)$. Degeneration corresponds to $\tau \to i\infty$ ($q = e^{2\pi i\tau} \to 0$), in which the minor-radius cycle collapses. $\mathbb{C}^\times = \mathbb{C} \setminus \{0\}$ arises as the infinite cylinder $\mathbb{C}/\mathbb{Z}$ with one end compactified. Cycle integrals: $\oint \epsilon_r^{11} = 1$, $\oint \epsilon_R^{22} = \tau \to i\infty$. At $\tau = i\infty$ the $D-1$ brane singularity forms.

Appendix D.3. Derivation of the Master Equation: Full Details

Starting from the energy-density relation $M_{\text{EW}}^2 = \rho_{\text{CY}} R_{\text{sing}}/M_{\text{Pl}}$ and $\rho_{\text{CY}} = T_{D-1}/V_{\text{sing}} = M_*^2/(g_s R_{\text{sing}}^3)$:

$$M_{\text{EW}}^2 = \frac{M_*^2}{g_s R_{\text{sing}}^3} \cdot \frac{R_{\text{sing}}}{M_{\text{Pl}}} = \frac{M_*^2}{g_s R_{\text{sing}}^2 M_{\text{Pl}}}. \tag{A23}$$

From $M_{\text{Pl}}^2 = M_*^8 R^6$: $M_{\text{Pl}} = M_*^4 R^3$, so

$$M_{\text{EW}}^2 = \frac{M_*^2}{g_s R_{\text{sing}}^2 M_*^4 R^3} = \frac{1}{g_s M_*^2 R^3 R_{\text{sing}}^2}. \tag{A24}$$

Taking the square root:

$$M_{\text{EW}} = \frac{1}{\sqrt{g_s}\, M_*\, R^{3/2} R_{\text{sing}}} = \frac{M_*}{\sqrt{g_s}} \cdot \frac{1}{(M_* R)^3 (M_* R_{\text{sing}})} = \frac{M_*}{\sqrt{g_s}} \cdot (M_*^4 R^3 R_{\text{sing}})^{-1}. \tag{A25}$$

 doi:10.20944/preprints202603.0916.v1

Now $M_*^4 R^3 R_{\text{sing}} = V_6^{1/2} R_{\text{sing}}^1 \cdot M_*^4 / M_*^0$ expressed in terms of volumes: writing $V_6 = R^6$ and $R_{\text{sing}} = (M_* R_{\text{sing}}) M_*^{-1}$:

$$(M_*^4 R^3 R_{\text{sing}}) = (V_6 R_{\text{sing}}^6)^{1/4} \cdot (\text{dimensionless factors}), \tag{A26}$$

which gives the master equation (64).

Appendix D.4. Supplemental Parameter Tables

Table A1. CY and brane parameters, $n = 6$, $M_* = 1\,\text{TeV}$, $g_s = 0.5$.

Quantity	Symbol	Value
Compact dimensions	n	6
CY volume	V_6	$R^6 \approx (4 \times 10^{-14})^6\,\text{m}^6$
Compactification radius	R	$4 \times 10^{-14}\,\text{m}$
Singularity radius	R_{sing}	$4 \times 10^{-29}\,\text{m}$
$M_* R$	—	$10^{5.3}$
Modular degeneration	τ	$i\infty$
Minor cycle	$\oint \epsilon_r^{11}$	1
NS intercept	α_{NS}	1/2
Critical dimension	P	10
Brane tension	T_{D-1}	$\sim M_*^2 / g_s$
First KK mass	$m_{\text{KK}}^{(1)}$	$\approx 30\,\text{MeV}$

Table A2. Lorentz generator mode assignments from Equation (41).

Assignment	Value	Consequence
$(P-2)/8 = 1$	$P = 10$	Critical dimension
$2\alpha_{NS} - (P-2)/8 = 0$	$\alpha_{NS} = 1/2$	NS intercept
$[L_{-i}, L_{-j}] = 0$	Algebra closes	No ghost states

Appendix E. Notation and Conventions: Extended Summary

This appendix collects additional notation and sign conventions used throughout the paper.

Index conventions.

- $M, N, \ldots \in \{0, 1, \ldots, 9\}$: ten-dimensional spacetime indices.
- $\mu, \nu, \ldots \in \{0, 1, 2, 3\}$: four-dimensional spacetime indices.
- $m, n, \ldots \in \{4, 5, \ldots, 9\}$: six compact-dimension indices.
- $a, b, \ldots \in \{1, \ldots, h^{1,1}\}$: Kähler moduli indices.
- $i, j, \ldots$: complex coordinates on the CY_3.

Metric signature.

We use the mostly-plus signature $(-, +, +, +, \ldots)$.

Natural units.

Throughout, $\hbar = c = k_B = 1$. Energies and masses are in GeV; lengths in m or GeV^{-1} (conversion: $1\,\text{GeV}^{-1} \approx 2 \times 10^{-16}\,\text{m}$).

 doi:10.20944/preprints202603.0916.v1

String conventions.

$\alpha' = \ell_s^2 = M_*^{-2}$. The string coupling $g_s = e^{\phi}$ where ϕ is the dilaton. In the Einstein frame, the Dp-brane tension is $T_{D(p)} = (2\pi)^{-p}\alpha'^{-(p+1)/2}g_s^{-1}$.

Differential form conventions.

p-form wedge products: $(\alpha \wedge \beta)_{\mu_1\ldots\mu_{p+q}} = \frac{(p+q)!}{p!q!}\alpha_{[\mu_1\ldots\mu_p}\beta_{\mu_{p+1}\ldots\mu_{p+q}]}$. The Hodge dual: $(*\alpha)_{\mu_{p+1}\ldots\mu_n} = \frac{1}{p!}\epsilon_{\mu_1\ldots\mu_n}\alpha^{\mu_1\ldots\mu_p}$.

Supersymmetry conventions.

We use the conventions of [10] for $\mathcal{N} = 1$ supergravity in four dimensions: the Kähler potential $\mathcal{K}$ has mass dimension 2, the superpotential W has mass dimension 3, and the scalar potential is $V = e^{\mathcal{K}/M_{\rm Pl}^2}(K^{i\bar{j}}D_iWD_{\bar{j}}\bar{W} - 3|W|^2/M_{\rm Pl}^2) + D$-terms.

References

1. N. Arkani-Hamed, S. Dimopoulos, and G. Dvali, "The hierarchy problem and new dimensions at a millimeter," *Phys. Lett. B* **429** (1998) 263–272.
2. N. Arkani-Hamed, S. Dimopoulos, and G. Dvali, "Phenomenology, astrophysics and cosmology of theories with sub-millimeter dimensions and TeV scale quantum gravity," *Phys. Rev. D* **59** (1999) 086004.
3. L. Randall and R. Sundrum, "A large mass hierarchy from a small extra dimension," *Phys. Rev. Lett.* **83** (1999) 3370–3373.
4. L. Randall and R. Sundrum, "An alternative to compactification," *Phys. Rev. Lett.* **83** (1999) 4690–4693.
5. P. Candelas, G. T. Horowitz, A. Strominger, and E. Witten, "Vacuum configurations for superstrings," *Nucl. Phys. B* **258** (1985) 46–74.
6. S. B. Giddings, S. Kachru, and J. Polchinski, "Hierarchies from fluxes in string compactifications," *Phys. Rev. D* **66** (2002) 106006.
7. S. Kachru, R. Kallosh, A. Linde, and S. P. Trivedi, "De Sitter vacua in string theory," *Phys. Rev. D* **68** (2003) 046005.
8. J. Polchinski, "Dirichlet-branes and Ramond-Ramond charges," *Phys. Rev. Lett.* **75** (1995) 4724–4727.
9. I. Antoniadis, "A possible new dimension at a few TeV," *Phys. Lett. B* **246** (1990) 377–384.
10. L. E. Ibáñez and A. M. Uranga, *String Theory and Particle Physics*. Cambridge University Press (2012).
11. E. G. Adelberger, B. R. Heckel, and A. E. Nelson, "Tests of the gravitational inverse-square law," *Annu. Rev. Nucl. Part. Sci.* **53** (2003) 77–121.
12. G. F. Giudice, R. Rattazzi, and J. D. Wells, "Quantum gravity and extra dimensions at high-energy colliders," *Nucl. Phys. B* **544** (1999) 3–38.
13. S.-T. Yau, "On the Ricci curvature of a compact Kähler manifold and the complex Monge–Ampère equation," *Commun. Pure Appl. Math.* **31** (1978) 339–411.
14. D. Bhattacharjee, "Generalization of quartic and quintic Calabi–Yau manifolds fibered by polarized K3 surfaces," (2022), `doi:10.21203/rs.3.rs-1965255/v1`.
15. D. Bhattacharjee, "M-theory and F-theory over theoretical analysis on cosmic strings and Calabi–Yau manifolds," *Asian J. Res. Rev. Phys.* (2022) 25–40.
16. D. McMahon, *String Theory Demystified*. McGraw-Hill, New York (2009).
17. A. Strominger, "Massless black holes and conifolds in string theory," *Nucl. Phys. B* **451** (1995) 96–108.
18. S. Gukov, C. Vafa, and E. Witten, "CFT and fields with ADE singularities," *Nucl. Phys. B* **584** (2000) 69–108.
19. G. 't Hooft, "Naturalness, chiral symmetry, and spontaneous chiral symmetry breaking," in *Recent Developments in Gauge Theories*, NATO Advanced Study Institutes Series **59** (1980) 135–157.
20. S. P. Martin, "A supersymmetry primer," *Adv. Ser. Direct. High Energy Phys.* **18** (1998) 1–98; updated version available as `arXiv:hep-ph/9709356`.

 doi:10.20944/preprints202603.0916.v1

21. ATLAS Collaboration, "Observation of a new particle in the search for the Standard Model Higgs boson with the ATLAS detector at the LHC," *Phys. Lett. B* **716** (2012) 1–29.
22. CMS Collaboration, "Observation of a new boson at a mass of 125 GeV with the CMS experiment at the LHC," *Phys. Lett. B* **716** (2012) 30–61.
23. ATLAS Collaboration, "Search for squarks and gluinos in final states with jets and missing transverse momentum at $\sqrt{s} = 13\,\text{TeV}$," *Eur. Phys. J. C* **81** (2021) 1111.
24. CMS Collaboration, "Searches for physics beyond the standard model with the M_{T2} variable in hadronic final states at $\sqrt{s} = 13\,\text{TeV}$," *J. High Energy Phys.* **05** (2021) 014.
25. ATLAS Collaboration, "Search for new resonances decaying to a W or Z boson and a Higgs boson in the $\ell^+\ell^- b\bar{b}$, $\ell\nu b\bar{b}$, and $\nu\bar{\nu}b\bar{b}$ channels in pp collisions at $\sqrt{s} = 13\,\text{TeV}$," *Phys. Lett. B* **798** (2019) 134949.
26. D. B. Kaplan and H. Georgi, "$SU(2) \times U(1)$ breaking by vacuum misalignment," *Phys. Lett. B* **136** (1984) 183–186.
27. N. Arkani-Hamed, A. G. Cohen, and H. Georgi, "Electroweak symmetry breaking from dimensional deconstruction," *Phys. Lett. B* **513** (2001) 232–240.
28. S. Weinberg, "Implications of dynamical symmetry breaking," *Phys. Rev. D* **13** (1976) 974–996.
29. L. Susskind, "Dynamics of spontaneous symmetry breaking in the Weinberg–Salam theory," *Phys. Rev. D* **20** (1979) 2619–2625.
30. P. W. Graham, D. E. Kaplan, and S. Rajendran, "Cosmological relaxation of the electroweak scale," *Phys. Rev. Lett.* **115** (2015) 221801.
31. W. D. Goldberger and M. B. Wise, "Modulus stabilization with bulk fields," *Phys. Rev. Lett.* **83** (1999) 4922–4925.
32. V. Balasubramanian, P. Berglund, J. P. Conlon, and F. Quevedo, "Systematics of moduli stabilisation in Calabi–Yau flux compactifications," *J. High Energy Phys.* **03** (2005) 007.
33. G. Panico and A. Wulzer, "The Composite Nambu–Goldstone Higgs," *Lect. Notes Phys.* **913** (2016) 1–316.
34. G. F. Giudice, "Naturally speaking: The naturalness criterion and physics beyond the standard model," in *Perspectives on LHC Physics*, World Scientific (2008) 155–178; `arXiv:0801.2562`.
35. J. E. Kim and H. P. Nilles, "The μ-problem and the strong CP problem," *Phys. Lett. B* **138** (1984) 150–154.
36. M. Berger, "Sur les groupes d'holonomie des variétés à connexion affine et des variétés riemanniennes," *Bull. Soc. Math. France* **83** (1955) 279–330.
37. P. Candelas and X. C. de la Ossa, "Comments on conifolds," *Nucl. Phys. B* **342** (1990) 246–268.
38. M. B. Stenzel, "Ricci-flat metrics on the complexification of a compact rank one symmetric space," *Manuscripta Math.* **80** (1993) 151–163.